國立臺灣大學醫學院分子醫學研究所

博士論文

Institute of Molecular Medicine

College of Medicine

National Taiwan University

Doctoral Dissertation

泛素接合酶 ZNRF1 藉由影響 caveolin-1 之代謝影響第四型類鐸受體驅動之免疫反應

The Ubiquitin Ligase ZNRF1 Promotes Caveolin-1 Ubiquitination and Degradation to Modulate TLR4-driven Immune Response

李志元

Chih-Yuan Lee

指導教授：徐立中 博士

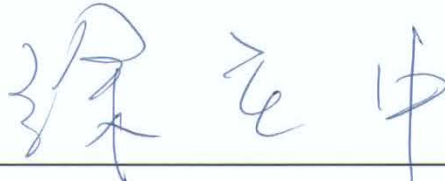Advisor: Li-Chung Hsu, Ph.D.

中華民國 106 年 01 月

January 2017

國立臺灣大學博士學位論文
口試委員會審定書

The Ubiquitin Ligase ZNRF1 Promotes Caveolin-1 Ubiquitination and Degradation to Modulate TLR4-driven Immune Response

泛素接合酶 ZNRF1 藉由影響 caveolin-1 之代謝影響第四型類鐸受體驅動之免疫反應

本論文係李志元君（學號 D97448005）在國立臺灣大學分子醫學研究所完成之博士學位論文，於民國 106 年 01 月 05 日承下列考試委員審查通過及口試及格，特此證明

口試委員：

_____（簽名）
（指導教授）

_____   _____

_____   _____

所長   _____（簽名）

1

中文摘要

　　泛素接合酶(ubiquitin E3 ligase)是一種蛋白酵素，它可以辨認並催化特定蛋白與泛素(ubiquitin)進行共價鍵結。泛素鍵結作用調控了許多各種不同的重要細胞功能，包括細胞週期的控制、細胞內蛋白質運送、DNA 修復、以及細胞內訊息傳導。在這篇研究裡面，主旨在研究泛素接合酶對於第四型類鐸受體(Toll-like receptor 4)訊息調控的影響。我們發現有一個泛素接合酶 ZNRF1 可以藉由影響另一個蛋白質 caveolin-1 (CAV1)來調控第四型類鐸受體受到刺激之後產生的免疫反應。我們也發現了 ZNRF1 與 CAV1 會有接觸與作用，在細胞受到脂多糖(lipopolysaccharide)的刺激後，ZNRF1 會催化 CAV1 接受泛素鍵結並促使 CAV1 在細胞內分解。CAV1 在細胞內是細胞小凹(caveolae)主要的組成蛋白並調控許多細胞生理功能以及變化,例如發炎反應以及癌細胞的生長。目前已之泛素鍵結作用可以影響 CAV1 在細胞內表現量的變化。我們的研究同時也發現 ZNRF1 與 CAV1 在第四型類鐸受體受到活化之後，會調控 Akt 與 GSK3β的功能來增加促進發炎反應細胞激素的分泌並且減少抑制發炎反應細胞激素的分泌。剔除 ZNRF1 基因的基因轉殖小鼠可以減少發炎反應並且剔除 ZNRF1 基因的基因轉殖小鼠對於內毒素(endotoxin)或是敗血症引起的休克有比較高的抵抗力以及存活率。我們的研究發現 ZNRF1 這個蛋白對於第四型類鐸受體引起的發炎反應是一個新的調控蛋白質,我們也發現了一個新的調控機制透過CAV1 來影響第四型類鐸受體引起的發炎反應。

　　關鍵字：ZNRF1，caveolin-1，TLR4，第四型類鐸受體。

Abstract

Ubiquitination catalyzed by E3 ligases are important enzymes in cell biology and regulate diverse cellular functions such as cell cycle control, protein trafficking, DNA repair, and signaling. Many E3 ubiquitin ligases have been characterized as important immune regulators. To characterize the molecular mechanisms underlying the immunoregulatory functions of these E3 ligases in physiologically relevant immune cells is still a challenge. Our research found that E3 ubiquitin ligase ZNRF1 modulates caveolin-1 (CAV1) protein stability to regulate Toll-like receptor (TLR) 4-triggered immune responses. We demonstrate that ZNRF1 interacts with CAV1 in response to lipopolysaccharides and mediates its ubiquitination and degradation. CAV1, the major constituent of caveolae, plays a pivotal role in various cellular physiological and pathological processes. The ubiquitin pathway is known to regulate the level of CAV1 in cells. Our research also found that ZNRF1-CAV1 axis regulates Akt-GSK3β activity upon TLR4 activation, resulting in enhanced production of pro-inflammatory cytokines and inhibition of anti-inflammatory cytokine. *Znrf1*-deficient mice are more resistant to endotoxic and polymicrobial septic shock due to attenuated inflammation. Our study has identified ZNRF1 as a new regulator of TLR4-induced inflammatory responses and revealed a novel mechanism for the regulation of TLR4 signaling through CAV1.

Key words: ZNRF1, caveolin-1, TLR4

Abbreviations

CAV1:   caveolin-1

NFκB: nuclear factor-κB

IκB: inhibitor of NF-κB

PRR: pattern-recognition receptor

TLR: toll-like receptor

PAMP: pathogen-associated molecular pattern

DAMP: danger-associated molecular pattern

LPS: lipopolysaccharide

MyD88:   myeloid differentiation primary response gene-88

MAPK: mitogen-activated protein kinase

IFN: interferon

TRIF: Toll/IL-1 receptor domain-containing adaptor-inducing interferon-β

TRAM: TRIF-related adaptor molecule

IRF3:   interferon regulatory factor 3

MHC: histocompatibility complex

IRAK: interleukin-1 receptor-associated kinase

ROS: reactive oxygen species

NADPH: nicotinamide adenine dinucleotide phosphate

4

EGFR: epidermal growth factor receptor

CLP: cecal ligation and puncture

BMDM: bone marrow-derived macrophage

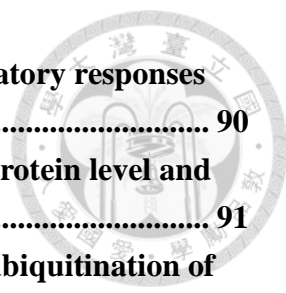M-CSF: macrophage colony-stimulating factor

目錄

Introduction

Inflammation is an important component of innate immunity and the host

response to pathogen infection. Excess activation of pro-inflammatory responses has

been associated with many inflammatory conditions, including atherosclerosis,

rheumatoid arthritis, and sepsis[1, 2]. Thus, the proper regulation of the inflammatory

response is fundamental for the treatment of inflammatory diseases[3, 4]. Ubiquitination

coordinates the activation of nuclear factor (NF)-κB, which is considered to be the

master mediator of inflammation and immune responses[5-7]. In this thesis, we studied the

role of an E3 ubiquitin ligase, ZNRF1, in the regulation of the inflammatory response.

1. Inflammation & Innate immunity

Most animals are capable of defending themselves from infectious pathogens by

activating their innate immunity. Upon infection, innate immune cells, including

macrophages and dendritic cells use pattern-recognition receptors (PRRs), mainly

Toll-like receptors (TLRs), to detect evolutionarily conserved microbial molecules

termed pathogen-associated molecular patterns (PAMPs), or danger-associated

molecular patterns (DAMPs), which are released from injured or dead cells[8]. The innate

immune cells then mount a defense response to clear the pathogen and damaged cells

and initiate intracellular signaling events leading to gene transcription of

pro-inflammatory cytokines to coordinate the adaptive immune response[9].
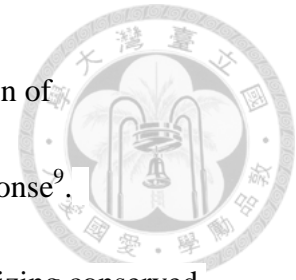
TLRs are crucial components of innate immunity. By recognizing conserved

pathogen components, TLRs activate specific signaling pathways and inflammatory

responses. The localization of TLRs dictates which adaptor proteins it interacts with and

subsequent downstream signaling and gene induction. Upon the binding of bacterial

lipopolysaccharides (LPS), TLR4 and MD2 are recruited to phosphatidylinositol

4,5-bisphosphate [PtdIns(4,5)P_2]-rich microdomains of the plasma membrane, where

TLR4 associates with myeloid differentiation primary response gene-88 (MyD88) via

the sorting adaptor MyD88-adaptor-like (Mal), leading to early IKK-NF-κB

and mitogen-activated protein kinase (MAPK) activation and the production of

pro-inflammatory cytokines[10, 11]. TLR4 and CD14 are then engulfed into the endosomal

compartment to trigger secondary signaling by recruiting Toll/IL-1 receptor

domain-containing adaptor-inducing IFNβ (TRIF) via the sorting adaptor TRIF-related

adaptor molecule (TRAM), resulting in interferon regulatory factor 3 (IRF3) activation

and the induction of type I interferon (IFN)[12]. TLR4 endocytosis is mediated by both

clathrin-dependent and lipid rafts/caveolae-dependent endocytic pathways[13]. However,

the molecular mechanism underlying the sorting of activated TLR4 and its downstream

signaling is not well understood.

2. Ubiquitination

Ubiquitination is a process of posttranslational modification of proteins that conjugates the small protein, ubiquitin, to substrates and is one of the most important pathways in eukaryotic cells. The protein substrates can be modified with a single ubiquitin or with a chain of many ubiquitins where one ubiquitin is connected to the next one. Ubiquitin is so named due to its ubiquitous expression pattern and is found in all eukaryotes[14]. Ubiquitination regulates a wide range of cellular processes, including cell cycle control, cell differentiation, DNA repair, transcriptional regulation and signal transduction[15]. Ubiquitination can act as a molecular signal marking the modified protein for degradation by the proteasome, a large multicatalytic protease. Ubiquitin-modified proteins are not always sent for destruction; indeed, many important non-proteolytic roles for ubiquitination of protein substrates have been reported, including regulating the subcellular localization, activity and function of the modified protein. Protein ubiquitination can also affect the interaction between transcription factors and co-activators, destine the localization of transcriptional activators and repressors, regulate the binding of transcription factors to target sites on chromatin, and determine the binding duration of transcription factors to promoters[11, 12]. Ubiquitin is activated in an ATP-dependent reaction and covalently conjugated to lysine residues in a

11
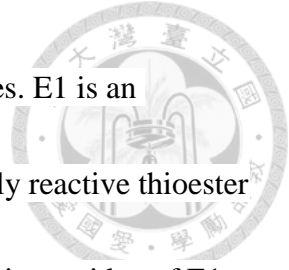
sequential three-enzyme cascade catalyzed by E1, E2 and E3 enzymes. E1 is an

ubiquitin activating enzyme, which catalyzes the formation of a highly reactive thioester

bond between the C-terminus glycine residue of ubiquitin and a cysteine residue of E1.

Ubiquitin is then transferred to the cysteine-containing active site of E2, an ubiquitin

conjugating enzyme, in a transthioesterification reaction to form an E2-ubiquitin

thioester intermediate. E3 is an ubiquitin ligase that catalyzes the formation of a

covalent bond between ubiquitin and a lysine residue on the substrate. The E3 ubiquitin

ligase binds to both the E2-ubiquitin intermediate and the substrate protein and then

catalyzes the ubiquitin from the E2-ubiquitin intermediate to form a covalent isopeptide

bond with a lysine residue in the substrate protein. Therefore, E3 ubiquitin ligases are

critical components that are specific to the ubiquitin system through their precise

interactions with the substrates.

Ubiquitin itself can also be ubiquitinated at one of its seven lysines to form

different types of polyubiquitin chains. Production of polyubiquitin chains involves

isopeptide bond formation between the carboxyl-terminal glycine residue of ubiquitin

and a lysine residue or the amino-terminal methionine of the ubiquitin conjugated to the

protein substrate. The presence of seven lysines (K) on the ubiquitin, along with the

amino-terminal methionine (M1), permit the formation of a family of multi-ubiquitin

chains, including the K6-, K11-, K27-, K29-, K33-, K48-, K63-, and M1-linked

12

poly-ubiquitin chains. The specificity of ubiquitination of protein substrates is mainly

determined by E3 ubiquitin ligases.

3. E3 ubiquitin ligases

E3 ubiquitin ligases bind to an E2-ubiquitin thioester intermediate and catalyze

the transfer of ubiquitin from the complex to a lysine residue on the substrate protein. It

was reported that there are more than 600 mammalian E3 ubiquitin ligases that

recognize protein substrates and assist in their ubiquitination[16, 17]. The E3 ubiquitin

ligases are classified into several families, including really interesting new gene (RING),

homology to E6AP C-terminus (HECT), RING-like (consisting of plant homeodomain/

leukemia-associated protein (PHD) and U-box) and the RING-between-RING (RBR)

family[14, 16, 17]. Each family of E3 ubiquitin ligase contains conserved domains. In

general, eukaryotic E3 ubiquitin ligases have either a HECT or a RING domain. RING

domains are characterized by conserved cysteines and histidines that bind Zn^{2+} ions to

stabilize   its structure for recognition and activation of E2 ubiquitin-conjugating

enzymes[18]. HECT domains are characterized on the basis of their conserved structure

that is similar to the C-terminal domain of the E6AP protein. In contrast to RING

domains, which could be found at any position within a protein, all HECT domains are

found at the C-terminus of the parent protein. RING-type E3 ubiquitin ligases could

13

bind different E2 ubiquitin-conjugating enzymes and have the potential to produce

several distinct types of poly-ubiquitin chains or mono-ubiquitination depending on the

E2 enzyme recruited[17]. In contrast, the HECT-type E3 ubiquitin ligase could only bind

to a specific substrate and the E2 enzyme determines the range of ubiquitin

modifications possible[19].

(1). HECT-type E3 Ubiquitin Ligases

The HECT-type E3 ubiquitin ligases have a highly conserved region of about

350 amino acids at the C-terminus, named the HECT domain[20]. The HECT domain has

a special bilobal structure: the N-lobe at the N-terminal end of the HECT domain serves

as the E2-binding site; whereas the C-lobe towards the C-terminus has a conserved

catalytically active cysteine residue, which forms a high-energy thioester bond with

ubiquitin and facilitates the transfer of ubiquitin to the substrate. The substrate

specificity of these HECT-type E3 ubiquitin ligases is determined by the N-terminal

segment of their respective proteins[20].

(2). RING-type E3 ligase

The RING-type E3 ligase has the consensus sequence of C3HC4 (C, cysteine; H,

14

histidine) or C3H2C3, which organizes two Zinc-binding sites. The RING-type E3

ligases bring the ubiquitin-E2 intermediates and the substrate into proximity, and

promote the transfer of ubiquitin directly from the complex to the protein substrates.
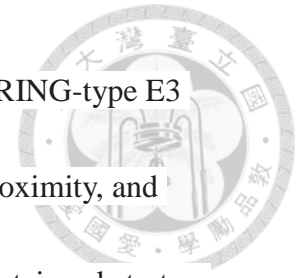
There are two general mechanisms by which ubiquitin are transferred to the protein

substrate. Unlike the HECT-type E3 ligases, which have an active cysteine residue at the

HECT domain for the binding and transfer of ubiquitin, RING-type E3 ubiquitin ligases

bind the E2 ubiquitin ligase and the substrate simultaneously to catalyze the direct

transfer of ubiquitin from the ubiquitin-E2 conjugating enzyme to the substrate. In

contrast, HECT and RBR ubiquitin ligases are involved in a two-step reaction in which

ubiquitin is first transferred from the E2 ubiquitin ligase to the E3 ubiquitin ligase to

form an E3-ubiquitin thioester conjugate, followed by transfer from this thioester

conjugate to a protein substrate[20, 21].

The RING-type E3 ubiquitin ligases are subdivided into single protein E3

ligases and multi-subunit E3 ligases depending on whether the functional RING domain

is present　as an entity in a single protein or as a subunit in a protein complex[22]. As

opposed to the former where the functional RING finger exists in a single protein, all

individual E3 ligases in the latter group have an approximately 100 amino acid-long

RING finger and a binding component to form a core enzymatic structure for the

recruitment of the E2-ubiquitin intermediate. Substrate recognition and recruitment is

mediated via another protein subunit.
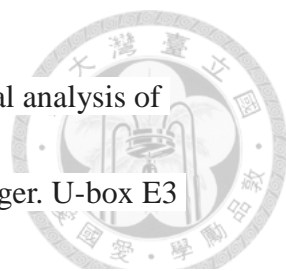
(3). PHD Domain-Containing E3 Ligases

The plant homeodomain (PHD) finger plays a role in ubiquitination and consists

of approximately 50-80 amino acids with a consensus C4HC3 zinc-binding sequence. It

belongs to the RING-like family of E3 ligases and possesses a configuration that is

similar in structure to yet different from the classical arrangement of a RING finger

domain[23,15]. The NMR structure of the PHD finger shows a globular fold with

conserved cysteine and histidine residues that can bind two Zn^{2+} ions. The PHD finger

is found in more than 400 eukaryotic proteins, many of which are involved in

transcriptional regulation and chromatin-mediated gene modulation.

(4). U-Box E3 Ligases

U-Box E3 ligases also belong to the RING-like family. U-Box E3 ligases were

originally identified as novel ubiquitination factors in yeast, known as UFD2 (ubiquitin

fusion degradation 2). Highly conserved homologues in other eukaryotes similar to

UFD2 have been demonstrated and consequently designated as U-box

(UFD2-homology domain). U-Box E3 ligases work together with another HECT-type

16

E3 ligase to facilitate assembly of longer ubiquitin chains[23]. Structural analysis of

U-box E3 ligases illustrates architectural similarities to the RING finger. U-box E3

ligases lack the typical zinc-binding cysteine or histidine residues as seen in the RING

finger for structural stabilization, instead, they are shown to utilize salt-bridges and

hydrogen bonds to form a RING-like structural scaffold[24]. The aromatic tryptophan

residues that are conserved in the RING finger and required for binding to E2 are also

found in the U-box E3 ligases[25].

(5). RING-between-RING (RBR) E3 ubiquitin ligase

RING-between-RING (RBR) E3 ubiquitin ligases also belong to the RING-like

family. They were originally identified by their RING domains; but the presence of

additional RING domains, in-between RING (IBR) and C-RING domains, characterized

them as a subclass of RING-type ubiquitin ligases[26]. RBR-type E3 ligases are

distinguished by three groups of specifically clustered cysteine and histidine residues

and   three adjacent domains: a canonical amino-terminal RING domain, N-RING,

which binds two zinc ions and folds into a classical RING domain; an in-between RING

domain (IBR); and another RING domain named C-RING, which binds only one zinc

ion[27]. RBR-type E3 ligases were classified into the RING-like family because of the

17
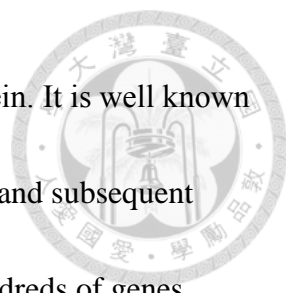
similarities between the N-RING domain and the canonical RING domains in both

structure and mechanism. However, since the cysteine residue in the C-RING domain

that is highly conserved among all RBR-type E3 ligases functions similarly to the active

cysteine site at the C-terminus of HECT-type E3 ligases, it was also proposed that

RBR-type E3 ligases could be perceived as RING-HECT hybrids[21].

E3 ubiquitin ligases are crucial enzymes in various aspects of cellular

homeostasis and functioning; therefore, we attempted to explore the role of an E3

ubiquitin ligase in innate immunity in this thesis.
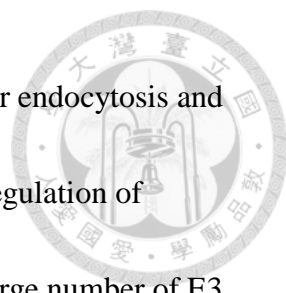
4. E3 Ubiquitin Ligase and Immune Response

Accumulated evidence clearly indicates that E3 ubiquitin ligases are involved in

the regulation of innate immune responses. The immune response usually involves the

initiation of gene transcription, which requires the assembly of many proteins, including

RNA polymerase II, transcription factors, and chromatin-modulating enzymes. The

roles of transcription factors in gene regulation are so critical that they are tightly

modulated via different mechanisms. One of the mechanisms is ubiquitin-dependent

proteolysis, which is involved in the regulation of many transcription factors, including

p53, c-Jun, and nuclear factor-κB (NF-κB). For example, NF-κB is maintained in an

18

inactive state through binding with an inhibitor of NF-κB (IκB) protein. It is well known

that the activation of NF-κB requires a critical step of ubiquitination and subsequent

degradation of IκB[28]. NF-κB is necessary for the transcription of hundreds of genes

involved in inflammation and immune homeostasis. The ubiquitination and proteasomal

degradation of cytoplasmic IκB proteins upon stimulation promote the transcriptional

activity of NF-κB. E3 ubiquitin ligases are also involved in the regulation of antigen

receptor-mediated signaling pathways and proteasomal-dependent processing of

antigenic peptides in antigen-presenting cells[24, 25]. E3 ligases are involved in various

aspects of both innate and adaptive immunity, such as the down-regulation of antigen

receptors, modulation of intracellular signaling molecules and transcription factors, and

antigen processing or expression.
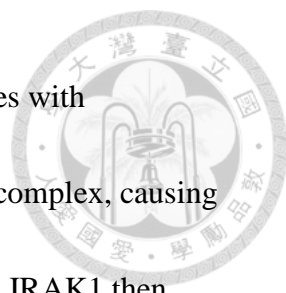
During an infection, dendritic cells recognize invading pathogens and are

stimulated to mature and become competent antigen-presenting cells, which present

microbial antigens to T cells and induce an efficient T cell response to clear the foreign

pathogens. Maturation of dendritic cells involves up-regulation of surface major

histocompatibility complex (MHC) class II and costimulatory molecules, including

CD80 and CD86[29]. An important mechanism that controls the surface expression of

MHC class II molecules and CD86 is ubiquitin-dependent degradation of these

molecules in the lysosome[30]. Membrane-bound RING-CH-1 (MARCH1) is an E3 ligase

19

that ubiquitinates MHC class II molecules and CD86, promoting their endocytosis and lysosomal degradation[31]. Therefore, ubiquitination is pivotal in the regulation of signaling pathways involved in the maturation of dendritic cells. A large number of E3 ubiquitin ligases have been characterized as prominent immune regulators that participate in different aspects of immune function, including TLR signaling in innate immunity, maturation of dendritic cells, and T cell activation. Ubiquitination does not always play a negative role in the functional regulation of its target proteins; occasionally, it activates kinase activity, protein-protein interaction, or gene transcription.

5. Ubiquitination in TLR Signaling
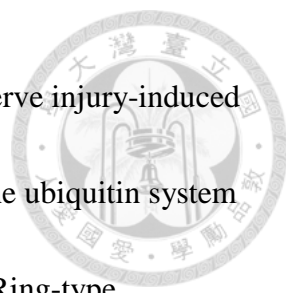
TLRs are a family of pattern-recognition receptors that are located on cell membranes and intracellular endosomal and lysosomal membranes. Surface-bound TLRs sense pathogens in the extracellular environment by recognizing membrane components of pathogens, whereas intracellular TLRs detect nucleic acids that have been internalized intracellularly through endocytosis or phagocytosis[32]. Signal transduction by TLRs relies on their association with specific adaptors. MyD88 is a common adaptor for all TLRs, except TLR3, whereas TRIF is an adaptor for TLR3 and

20

TLR4. Upon activation, MyD88 is recruited to the TLR and assembles with

interleukin-1 receptor-associated kinase (IRAK)4 and IRAK1 into a complex, causing

activation of IRAK4 and phosphorylation of IRAK1. Phosphorylated IRAK1 then

activates TRAF6, which functions as both an adaptor and an E3 ubiquitin ligase that

catalyzes the formation of K63-linked poly-ubiquitin chains involving TRAF6 itself and

other proteins. TRAF6 also activates the ubiquitin-dependent kinase TAK1, which in

turn activates IKK, JNK, ERK and p38.   This signaling pathway eventually leads to

the induction of transcription factors and pro-inflammatory cytokines. In response to

TLR3 and TLR4 activation, TRIF recruits RIP1 and stimulates its K63-linked

poly-ubiquitination, which is important for the recruitment and activation of TAK1.

TRIF also activates the IKK-related kinases TBK1 and its homologue IKKε, resulting in

the induction of the transcription factor IRF3 and type I IFNs. Ubiquitination plays a

critical role in the regulation of signal transduction in relation to TBK1 and IKKε[33, 34].
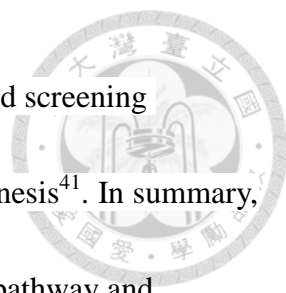
6. ZNRF1

It is recognized that one E3 ubiquitin ligase, zinc and ring finger 1 (ZNRF1), is

up-regulated in macrophages upon LPS exposure. Nevertheless, the exact function of

ZNRF1 in macrophages and TLR signaling remains unknown. In this study, we tried to

investigate the role of E3 ubiquitin ligase in TLR4 signaling and found that a

21

RING-type E3 ubiquitin ligase, ZNRF1 (previously identified as a nerve injury-induced gene[35]), promotes CAV1 degradation during inflammation through the ubiquitin system and also affects TLR4 signaling. ZNRF1 is a protein that contains a Ring-type zinc-finger motif and is constitutively expressed in neurons during development. The role of ZNRF1 in TLR4 signaling and the inflammatory response is still unknown. The Ring-type zinc-finger motif is a zinc-binding domain that functions as a ubiquitin E3 ligase. A cysteine to alanine mutation at amino acid 184 in the RING domain of *Znrf1* will lead to loss of E3 ligase activity[36, 37].

It was reported that reactive oxygen species (ROS) generated by nicotinamide adenine dinucleotide phosphate (NADPH) oxidases would serve as an intracellular signaling mediator to activate epidermal growth factor receptor (EGFR)-dependent phosphorylation of ZNRF1, thereby turning on its ubiquitin ligase activity and promoting ubiquitination of AKT[38]. They proposed that the ZNRF1–AKT–glycogen synthase kinase 3B (GSK3B)–collapsin response mediator protein 2 (CRMP2) pathway would promote axonal degeneration after neuronal injury. ROS trigger ZNRF1 activity and turn on pathways that induce neuronal apoptosis and axonal degeneration. Inhibition of NADPH oxidase activity would result in ZNRF1 downregulation and thus inhibition of oxidative stress-induced neuronal apoptosis[39]. It was also reported that ZNRF1 would interact with the α1 subunit of Na^+/K^+ATPase and mediate its

22
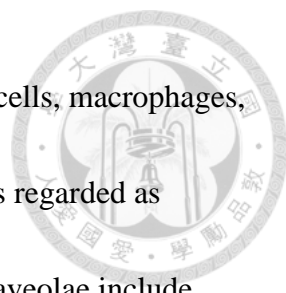
ubiquitination[40]. Furthermore, it was identified using yeast two-hybrid screening

that ZNRF1 interacts with beta-tubulin type 2 and regulates neurogenesis[41]. In summary,

ZNRF1 is activated by ROS in the ZNRF1–AKT–GSK3B–CRMP2 pathway and

interacts with beta-tubulin type 2; however, the function of ZNRF1 in the immune

system remains unclear.

We discovered that, in macrophages, ZNRF1 associates with and promotes

degradation of CAV1 upon TLR4 activation. The depletion of ZNRF1 in macrophages

leads to increased PI3K-Akt activity in response to LPS, which then blocks GSK3β

activation, resulting in an attenuation of gene expression related to inflammation and

induction of the anti-inflammatory cytokine IL-10. In addition, mice with a

myeloid-specific-deletion of ZNRF1 are significantly resistant to both LPS- and cecal

ligation and puncture (CLP)-induced sepsis and exhibit a reduced inflammatory

response, demonstrating the positive regulatory role of ZNRF1 in TLR4-driven

inflammation. Our results collectively reveal ZNRF1 as a novel regulator of the TLR4

signaling pathway through control of CAV1 protein stability.

7. Caveolae and Inflammatory Signaling

Caveolae, a special subset of lipid rafts rich in cholesterol and sphingolipids, are

small, flask-shaped invaginations (60-80 μm in diameter) of the plasma membrane.

23

Caveolae are ubiquitous in various cell types, including endothelial cells, macrophages,

and adipocytes. Lipid rafts are higher-order membrane microdomains regarded as

assemblies of glycosphingolipids and cholesterol. The functions of caveolae include

endocytosis, phagocytosis, sorting of vesicles, and   regulation of various signaling

pathways[42]. The major constituent of caveolae is the caveolin-1 (CAV1) protein, which

is essential for caveola biogenesis and regulation of caveola-mediated cellular

functions[43]. There are three isoforms of caveolin, namely caveolin-1, 2, and 3. CAV-1

and 2 are expressed in various cell types, whereas CAV-3 is muscle-specific. CAV1

serves as a regulator of diverse cellular signaling pathways[44]. Given the importance of

CAV1 in caveola formation and cellular functioning, the regulation of CAV1 expression

has been the subject of extensive study. However, most of these studies have focused on

the function of CAV1 in endocytosis, while its role in the immune response remains to

be identified.

Caveolae or caveolin have been identified in macrophages, mast cells,

neutrophils, lymphocytes, monocytes and dendritic cells[45, 46]. Accumulating evidence

indicate that lipid rafts/caveolae play an important role in the signaling pathways

involved in the activation of both innate and adaptive immune responses[47]. TLR2 and

TLR4 were shown to translocate to lipid rafts where they assemble with the adaptor

protein Mal-MyD88 and downstream signaling molecules upon ligand binding[44, 48].

24

Wang et al. reported that over-expression of CAV1 decreases LPS-induced TNF and

IL-6 production and augments IL-10 generation in LPS-challenged murine peritoneal

macrophages and RAW264.7 cells[49]. In another report, over-expression of CAV1 was

also shown to exert anti-inflammatory effects in response to LPS, although the

underlying mechanism was inconclusive[50]. Different studies have reported distinct

findings, especially in animal models of sepsis, which suggests that the roles of

caveolae and CAV1 in the regulation of inflammation and sepsis are complex.

In this study, our research aims to investigate the effect of E3 ubiquitin ligase on

TLR signaling and we found that a RING-type E3 ubiquitin ligase, ZNRF1, promotes

CAV1 degradation during inflammation through the ubiquitin system and influences

TLR4 signaling.

25

Purpose of the Study

The immune response usually involves gene transcription, which requires the assembly of many proteins, including RNA polymerase II, transcription factors, and chromotin-modulating enzymes. The roles of transcription factors in gene expression are so critical that they are stringently regulated by different mechanisms. One of these is ubiquitination, and E3 ubiquitin ligases are involved in coordinating these innate immune processes. An ubiquitin E3 ligase is a protein that recognizes a protein substrate, and catalyzes the transfer of ubiquitin to that substrate. Ubiquitination by E3 ligases is critical in cellular metabolism and regulates diverse functions such as cell cycle control, protein trafficking, DNA repair, and signaling. E3 ubiquitin ligases are also involved in the regulation of antigen receptor-mediated signaling pathways and proteasome-dependent processing of antigenic peptides in antigen-presenting cells. In this study, we attempted to study the effect of E3 ubiquitin ligase on TLR signaling. More specifically, since zinc and ring finger 1 (ZNRF1), a RING-type E3 ubiquitin ligase, has been previously shown to regulate TLR4-triggered immune response, our current study continued to delineate its underlying mechanism and its physiological function *in vivo*.

Material and Methods
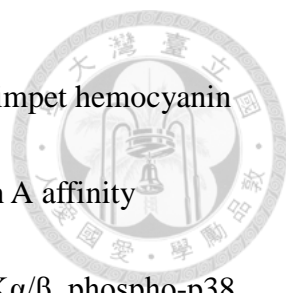
Plasmids

Full-length ZNRF1 and ZNRF2 cDNAs were amplified by PCR from a mixture of cDNAs derived from C57BL/6 mouse livers and cloned into pcDNA3 (Invitrogen, Carlsbad, CA) containing a C-terminal Flag epitope tag. A plasmid encoding Flag-tagged ZNRF1 (C184A) mutant was generated by site-directed mutagenesis using the QuickChange II Site-Directed Mutagenesis Kit (Stratagene, La Jolla, CA). Flag-ZNRF1 and Flag-ZNRF1(C184A) were subsequently cloned into the pLKO-AS2 lentivirus-based vector (National RNAi Core Facility, Academia Sinica, Taiwan) for lentivirus production. CAV1 cDNA was PCR amplified and cloned into a pLKO-AS2 lentiviral vector with V5-tagged C-terminal. The CAV1 and ZNRF1 deletion mutants were generated by PCR using full-length CAV1 and ZNRF1 as templates. All mutations were confirmed by DNA sequencing. The pcDNA-HA-Ubiquitin plasmid was obtained from Addgene (Cambridge, MA).

Reagents and Antibodies

Anti-ZNRF1 polyclonal antibodies was generated in rabbits immunized with a synthetic peptide corresponding to amino acids 71-86 (amino acid sequence

27

LYTPASRGTGDSERAP) of human ZNRF1 conjugated to keyhole limpet hemocyanin

(KLH). Rabbit antisera were collected and further purified by Protein A affinity

chromatography. Antibodies against P65, GAPDH, H3, phospho-IKKα/β, phospho-p38,

phospho-JNK1/2, phospho-ERK1/2, IKKα/β, p38, JNK1/2, ERK1/2, CAV1,

phospho-GSK3β (Ser9), phospho-AKT (Ser473), GSK3β, and AKT were obtained from

Cell Signaling Technology (Danvers, MA). The anti-c-Jun and anti-phospho-CREB

(Ser129) antibodies were received from Santa Cruz Biotechnology (Santa Cruz, CA)

and anti-β-actin antibody was procured from Millipore (Billerica, MA). The

anti-ubiquitin and ZNRF2 antibodies were purchased from Covance (Princeton, NJ) and

Abcam (Cambridge, UK), respectively. Antibodies against V5 and HA and

anti-Flag-conjugated Sepharose were provided by Bethyl Laboratories (Montgomery,

TX). The anti-Flag and anti-CD68 antibodies were obtained from BioLegend (San

Diego, CA) and Proteintech (Chicago, IL). High-molecular-weight (HMW)

polyinosinic-polycytidylic acid (poly(I:C)) and macrophage colony-stimulating factor

were received from InvivoGen (San Diego, CA) and Peprotech (Rocky Hill, NJ),

respectively. All other chemicals, including LPS (*Escherichia coli* 0111:B4), were

purchased from Sigma-Aldrich (St. Louis, MO).
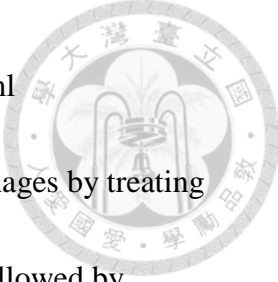
Mice

Znrf1[F/F] mice were generated via two homologous recombination events in embryonic stem cells (ES cells) where two *loxP* sites were inserted into the first and third introns of the *Znrf1* gene because of the long second intron. To generate hematopoietic cell-specific *Znrf1*-deletion mice, we crossed *Znrf1*[F/F] mice with interferon-inducible Mx1 promoter-driven Cre recombinase transgenic mice[51]. To delete *Znrf1* in *Znrf1*[F/F]:*Mx1-Cre* mice, 3- to 4-week-old mice were injected intraperitoneally with 10 μg/g poly(I:C) twice every other day; the mice were used in experiments 2 weeks later. These mice are referred to as *Znrf1*[Δ] mice. C57BL/6 mice were obtained from the Animal Center of the National Taiwan University Medical College. *Znrf1*[F/F] mice were backcrossed with C57BL/6 mice for at least 9 generations and housed in a specific-pathogen-free animal facility. All animal experiments were conducted in accordance with animal welfare guidelines and were approved by the Institutional Animal Care and Use Committee (IACUC) of the College of Medicine, National Taiwan University (approval no. 20120220).

Cell Cultures and BMDM Preparation
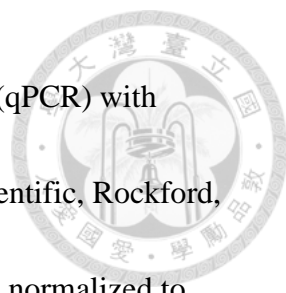
Murine macrophage-like RAW264.7 cells and human promonocytic leukemia cell THP-1 were cultured in RPMI 1640 (Hyclone, Logan, UT) supplemented with

29

10% (vol/vol) heat-inactivated fetal bovine serum (FBS) and 100 U/ml

penicillin/streptomycin. THP-1 cells were differentiated into macrophages by treating

cells with 25 ng/ml of phorbol 12-myristate 13-acetate for 4 hours, followed by

overnight incubation in fresh medium before commencing experiments. Human

embryonic kidney HEK293T cells were cultured in DMEM containing 10% FBS

and 100 U/ml penicillin/streptomycin. Bone marrow from 6- to 8-week-old mice was

used to prepare bone marrow-derived macrophages (BMDMs). BMDMs were prepared

as dictated previously[52]. Briefly, femurs and tibia bones were collected from mice, and

bone marrow was flushed out with DMEM medium using a 25-gauge syringe. The bone

marrow cells were harvested, and cultured in high-glucose DMEM medium

supplemented with 20% L929 cell-conditioned medium for 7 days to differentiate into

macrophages. BMDMs were collected and cultured in DMEM containing 10 ng/ml

macrophage colony-stimulating factor (M-CSF) (Peprotech, Rocky Hill, NJ) for further

experiments.

mRNA Purification and Quantitative RT-PCR (RT-qPCR)

Total cellular RNA was isolated with RNeasy® Mini Kit (Qiagen, Valencia, CA) and

used to synthesize cDNA with RevertAid H Minus First Strand cDNA Synthesis Kit

(Thermo Scientific, Rockford, IL) according to the manufacturer's instructions. The
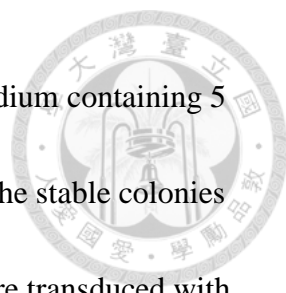
quantity of cDNA was measured using real-time quantitative PCR (qPCR) with

Maxima® SYBR Green/Fluorescein qPCR Master Mix (Thermo Scientific, Rockford,

IL) as per manufacturer's recommendations. All qPCR values were normalized to

cyclophilin mRNA levels to obtain the relative values. All experiments were performed

in triplicate. The primer sequences are shown in Table 2.

shRNA-Mediated Gene Silencing, Transfection, and Lentiviral Infection

Lentiviral shRNA constructs encoding short hairpin RNAs (shRNAs) against mouse

Znrf1 in pLKO-puro vectors (pLKO-shZnrf1) were obtained from the National RNAi

Core Facility Platform at the Institute of Molecular Biology/Genomic Research Center,

Academia Sinica, Taiwan. The target sequences were

5'-CATGGTTTGAAGTGAACAGAT-3' for *Znrf1* shRNA 1,

5'-GAGATGGAAATGCACTTTATA-3' for *Znrf1* shRNA2, and 5'-

GATGAAATGGATTTGCATCTT-3' for *Znrf2* shRNA. HEK293T cells were transfected

with pLKO-shRNA constructs and the packaging plasmids pMD.G and pCMVR8.91

using Turbofect (Fermentas, Schwerte, Germany) based on the manufacturer's

directions. Culture medium containing the lentivirus was collected 48 and 72 hours after

transfection. RAW264.7 and THP-1 cells were infected overnight with lentiviruses in

the presence of 8 µg/ml polybrene (Sigma-Aldrich, St. Louis, MO) and cultured in fresh

medium for another 24 hours. The infected cells were selected in medium containing 5 µg/ml puromycin until the uninfected cells were completely killed. The stable colonies were pooled together for further experiments. Bone marrow cells were transduced with shRNA-encoding lentiviruses on days one and two of differentiation into macrophages as described previously[53].

siRNA Duplexes and Electroporation

Predesigned siRNA against mouse *Cav1* (5′-GCAAAUUUAUGAAUGGUUUdTdT-3′), and the negative control siRNA (5′-GAUCAUACGUGCGAUCAGA dTdT-3′) were obtained from Sigma-Aldrich (St. Louis, MO). BMDMs were electroporated with 100 nM siRNA duplexes using the Neon transfection system (Invitrogen) according to the manufacturer's instructions. Briefly, 5×10^5 cells were electroporated with two 30 ms pulses at 1,500 V, and were cultured for another 48 hours before further experiments.

Enzyme-Linked Immunoabsorbent Assays (ELISA) and Myeloperoxidase (MPO) Activity Assay

The levels of cytokines and chemokines in sera and culture supernatants were

measured using DuoSet ELISA systems (R&D Systems, Minneapolis, MN) as per

manufacturer's recommendations.   MPO activity in mouse lung homogenates was

determined using the MPO colorimetric assay (BioVision, Milpitas, CA) by following

the manufacturer's instructions.
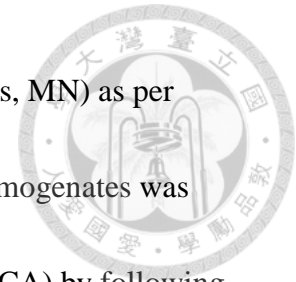
Immunoprecipitation and Immunoblotting

   Whole cells were harvested and lysed in ice-cold lysis buffer containing 150 mM

NaCl, 20 mM Tris-HCl pH 7.4, 0.5% Triton X-100 and protease inhibitor cocktail

(Roche, Basel, Switzerland) and were homogenized by sonication in 1.5-ml microfuge

tubes on ice for 30 seconds. Protein concentrations were determined using the Bradford

assay (Bio-Rad, Hercules, CA). Cellular extracts (200 μg) were incubated with the

indicated antibody overnight, followed by an 1-hour incubation with Protein A/G beads

or antibody-conjugated beads overnight at 4°C. The immunocomplexes were separated

by SDS-PAGE and transferred to nitrocellulose membranes. The membranes were then

incubated with the indicated primary antibody followed by an HRP-conjugated

secondary antibody. Immunoreactive bands were detected using Western Lighting®

Plus-ECL (PerkinElmer, Waltham, MA).

InVitro Ubiquitination Assay

Recombinant His-ZNRF1-Flag, His-ZNRF1(C184A)-Flag, and His-CAV1-V5 proteins were expressed in *Escherichia coli* BL21, and purified using Ni-nitrilotriacetic acid (Ni-NTA) resins (Macherey-Nagel, Düren, Germany) by following manufacturer's recommendations. Specific E1 and E2 were obtained from Enzo Life Sciences (Farmingdale, NY). *In vitro* ubiquitination assays were performed by incubating 500 ng His-tagged ZNRF1-Flag or ZNRF1(C184A)-Flag, and 500 ng His-CAV1-V5 together with 1 μg ubiquitin (Boston Biochem, Cambridge, MA), 100 ng His–Ube1, and 150 ng His–UbcH5c in the reaction buffer (25 mM Tris-HCl pH 8.0, 100 mM NaCl, 1 mM DTT, 1 mM $MgCl_2$, 100 μM $ZnSO_4$, 2 mM ATP), at 30°C for 3 hours. The reactions were terminated by adding lysis buffer (150 mM NaCl, 20 mM Tris-HCl pH 7.4, 1% SDS) and subjected to immunoblotting.

PP2A Activity Measurement

Cells were lysed in the lysis buffer containing 50 nM Tris-HCl pH7.4, 150 mM NaCl, 1 mM EDTA, 1% Triton-X100 and protease inhibitor. Cell lysates were immunoprecipitated with antibody against PP2A catalytic subunit for 2 hours. The immunoprecipitants were subjected to PP2A phosphatase activity assay using the PP2A Immunoprecipitation Phosphatase assay kit (Millipore, Billerica, MA) according to the
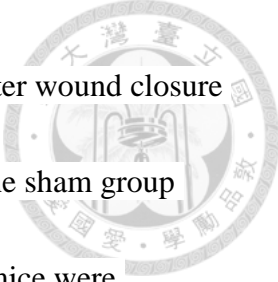
34

manufacturer's instructions.

In Vivo Administration of siRNAs

siRNA was delivered *in vivo* using *in vivo*-jetPEI^{TM} (Polyplus-transfection, Illkirch,

France) in keeping with the manufacturer's protocols. In brief, 40 µg siRNA duplex was

mixed with 6.4 µl *in vivo*-jetPEI in a final volume of 200 µl of 10% glucose. The

mixture was incubated for 15 minutes at room temperature and was delivered to the

mice by intravenous injection into the femoral vein.

Animal Models of Endotoxemia and Polymicrobial Sepsis

To induce endotoxemia, age- and weight-matched male *Znrf1*$^{F/F}$ and *Znrf1*$^{\Delta}$ mice were

injected intraperitoneally with bacterial endotoxin (LPS; 15 mg/kg). Blood samples

were collected 6 hours after LPS challenge, and serum cytokines were measured using

ELISA. Polymicrobial sepsis was induced by CLP as previously described[52]. Briefly,

mice were anesthetized and maintained with isoflurane, and a 2-cm midline laparotomy

was performed to allow the exposure of the cecum and the adjacent intestine. A 3-0 silk

suture was used to tightly ligate the cecum at its base below the ileocecal valve, and the

cecum was punctured once with a 21-gauge needle. The cecum was then gently returned

to the peritoneal cavity. The laparotomy was closed with a 5-0 silk suture. All mice were

subcutaneously injected with sterile saline (50 ml/kg) immediately after wound closure

and placed in cages with free access to food and water. The mice in the sham group

underwent the same surgical procedures except CLP. After CLP, the mice were

monitored for survival for 7 days. In a different set of experiments, blood and tissues

were collected for cytokine measurements and histological analysis 4 and 8 hours after

CLP, respectively.

Statistical Analysis
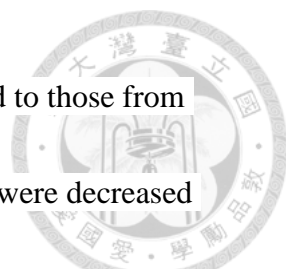
The results are presented as mean±SD. Statistical significance of differences

between groups was determined using Student's t-test. The log-rank test was used to

compare differences between survival curves. P values less than 0.05 were considered
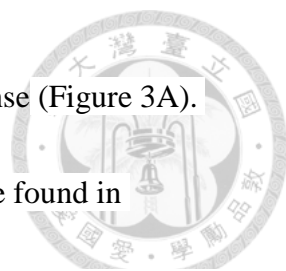
statistically significant.

Results

ZNRF1 is involved in the Regulation of TLR4-driven Inflammatory Response in Macrophages

We explored the GDS2047 microarray dataset in the publicly accessible microarray database of the National Center for Biotechnology Information and identified that an E3 ubiquitin ligase, ZNRF1, was upregulated in macrophages upon LPS stimulation. To further explore the function of ZNRF1 in macrophages during inflammation, we generated $Znrf1^{F/F}$ ($loxP$-flanked $Znrf1$) mice by inserting two $loxP$ sites into the first and third introns of the $Znrf1$ gene through two sequential rounds of homologous recombination (Figure 1A). $Znrf1^{F/F}$ mice were crossed with transgenic mice in which Cre recombinase was driven by an IFN-inducible Mx1 promoter. We deleted the $Znrf1$ gene in cells of the myeloid lineage by administering polyinosinic-polycytidylic acid [poly(I:C)] to mice (called '$Znrf1^{\Delta}$' here). As a control, $Znrf1^{F/F}$ mice received the same poly(I:C) administration schedule (Figure 1B, C). Bone marrow cells isolated from either $Znrf1^{\Delta}$ or $Znrf1^{F/F}$ mice were differentiated into macrophages (BMDMs). Blood counts from both groups demonstrated no obvious difference (Table 1).

Expression of cytokine mRNA from ZNRF1 depleted BMDMs was significantly inhibited, including TNF, IL-6, IL-1β, CCL5 and IFNβ. In the meantime, IL-10 mRNA

37

was elevated in LPS-stimulated BMDMs from $Znrf1^{\Delta}$ mice compared to those from

$Znrf1^{F/F}$ mice (Figure 2A). Accordingly, TNF, IL-6 and CCL5 levels were decreased

while IL-10 was increased in $Znrf1^{\Delta}$ BMDMs after LPS treatment (Fig. 2B). Stimulation

of macrophages by LPS leads to MAPK activation in a MyD88 dependent fashion. The

activation of MAPK in both $Znrf1^{F/F}$ and $Znrf1^{\Delta}$ isolated BMDMs was also examined.

Surprisingly, despite slightly increased p38 activation, LPS-induced activation of

IKKα/β and MAPKs, JNK and ERK, was not significantly different between $Znrf1^{F/F}$

and ZNRF1-deficient BMDMs (Figure 2C). In addition, ZNRF1-depleted macrophages

exhibited a modest increase in the phosphorylation of IRF3 in response to LPS.

The cysteine residue at position 184 in the RING finger domain of ZNRF1 is

reportedly critical for its E3 ubiquitin ligase activity[34]. To determine if the E3 ubiquitin

ligase activity of ZNRF1 is required for the modulation of TLR4-driven immune

responses, we examined the induction of gene expression by LPS in $Znrf1^{\Delta}$ BMDMs

reconstituted with either wild-type ZNRF1 or a catalytically inactive E3 ligase mutant

ZNRF1 (C184A). It was found that the LPS-induced *Tnf, Il6* and *Il1b* mRNA levels

were increased in BMDMs after reconstitution with ZNRF1 but not in those

reconstituted with the ZNRF1 (C184A) mutant. By contrast, *Il10* mRNA was

downregulated in the ZNRF1-reconstituted BMDMs but not in those reconstituted with

the ZNRF1 (C184A) mutant, suggesting a requirement of its E3 ubiquitin ligase activity
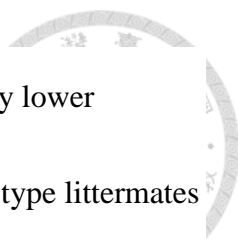
38

in the ZNRF1-mediated effects on the TLR4-induced immune response (Figure 3A).

Accordingly, elevated TNF and IL-6 and decreased IL-10 levels were found in

supernatants of BMDMs reconstituted with ZNRF1 but not in those reconstituted with

ZNRF1 (C184A) mutant after stimulation with LPS (Figure 3B). These results indicate

that ZNRF1 is involved in the regulation of cytokine production after TLR4 activation

and the depletion of ZNRF1 impedes the coordination of cytokine synthesis in

macrophages. These data confirm an important role for ZNRF1 in overseeing

TLR4-induced pro-inflammatory cytokine production in macrophages, and the fact that

this relies on ZNRF1's ubiquitin ligase activity advocates a novel mechanism for the

regulation of TLR4 signaling.

Depletion of ZNRF1 in myeloid cells Protects Mice from CLP- and LPS-induced

Septic Shock

Sepsis has been attributed to an exorbitant release of pro-inflammatory cytokines

that results in high morbidity and mortality[54]. We assessed the physiological role of

ZNRF1 in modulating inflammatory responses and septic shock *in vivo*

by intraperitoneally injecting $Znrf1^{\Delta}$ and control mice with a lethal dose of LPS. After

LPS challenge, more than 50% of wild-type mice died within 48 hours whereas more

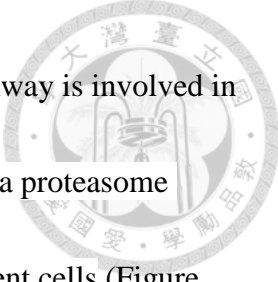than 60% of $Znrf1^{\Delta}$ mice survived for up to 72 hours (Figure 4A). The serum

39

concentrations of TNF, IL-6 and IL-1β induced by LPS were significantly lower

whereas IL-10 levels were higher in $Znrf1^\Delta$ mice compared to their wild-type littermates

(Figure 4B). These results suggest that decreased plasma concentrations of

pro-inflammatory cytokines contribute to the greater resistance of the $Znrf1^\Delta$ mice to

endotoxins. In addition, we evaluated the effect of $Znrf1$ deficiency on septic shock

using the CLP model, a clinically relevant rodent model of polymicrobial sepsis.

Consistent with the results of LPS-induced sepsis, the survival rate of $Znrf1^\Delta$ mice was

higher than that of $Znrf1^{F/F}$ mice (Figure 5A). The serum levels of TNF, IL-6 and IL-1β

after CLP were also lower in $Znrf1^\Delta$ mice than in $Znrf1^{F/F}$ mice, whereas IL-10

expression was slightly higher in the $Znrf1^\Delta$ group (Figure 5B). Other pro-inflammatory

cytokines and chemokines, including IL-12p40, MCP-1, MIP-1α and CCL5, were also

markedly decreased in CLP-treated $Znrf1^\Delta$ mice (Figure 6). Histological analysis

revealed significantly less inflammation and edema in lung tissue from $Znrf1^\Delta$ mice

compared to $Znrf1^{F/F}$ mice after CLP (Figure 7A). In line with less pulmonary

inflammation, myeloperoxidase activity, the neutrophil marker, was decreased in lung

homogenates from CLP-challenged $Znrf1^\Delta$ mice (Figure 7B). In addition, the quantity of

liver infiltrating macrophages was lower in CLP-treated $Znrf1^\Delta$ mice than in control

mice (Figure 7C). These results collectively demonstrate that ZNRF1 is a critical

regulator of pro-inflammatory cytokine production during sepsis with a significant

impact on mortality.

ZNRF1 Mediates CAV1 Protein Degradation

The pattern of cytokine production observed after LPS treatment

in $Znrf1^{\Delta}$ BMDMs in this study, i.e., suppressed induction of the pro-inflammatory

cytokines TNF and IL-6 and elevated production of the anti-inflammatory cytokine

IL-10, is similar to that reported in CAV1-overexpressing macrophages[55] and dendritic

cells[56]. In addition, we consistently observed significantly higher CAV1 protein

expression in livers from $Znrf1^{\Delta}$ mice after CLP challenge compared to littermate

controls (Figure 8A, B). An effort had thus been made to examine CAV1 protein levels

in ZNRF1-depleted macrophages. CAV1 protein levels were significantly increased in

ZNRF1-deficient BMDMs, and this increase was even more prominent after LPS

stimulation (Figure 9A). This observation implies that ZNRF1 might suppress the

expression of CAV1 after TLR4 activation. To verify this, we stably expressed

Flag-tagged ZNRF1 and examined CAV1 expression accordingly. CAV1 protein was

decreased when ZNRF1 was overexpressed in the RAW264.7 murine macrophage cell

line (Figure 9B), indicating that CAV1 levels   are   modulated by ZNRF1. CAV1

protein degradation is reportedly dependent on both the ubiquitin/proteasomal and

41

endolysosomal pathways. Therefore, we further examined which pathway is involved in

ZNRF1-regulated CAV1 protein stability. Pretreatment with MG132, a proteasome

inhibitor, restored CAV1 levels in control cells but not ZNRF1-deficient cells (Figure

10A). However, the lysosome inhibitors NH_4Cl and chloroquine had a partial inhibitory

effect on CAV1 degradation in both control and ZNRF1-silenced cells (Figure 10B). To

determine if ubiquitination is required for ZNRF1-controlled CAV1 expression, we

expressed either wild-type ZNRF1 or the catalytically inactive E3 ubiquitin ligase

mutant ZNRF1 (C184A) in HEK293T cells. The levels of endogenous CAV1 were

gradually reduced in cells expressing increasing amounts of ZNRF1 but not in cells

expressing ZNRF1 (C184A) (Figure 11). Similarly, the suppression effect of ZNRF1

was abolished in cells pretreated with MG132. ZNRF2 is a close structural homologue

of ZNRF1. To examine the regulatory effect of ZNRF2 on CAV1 protein stability, we

expressed ZNRF2 in HEK293T cells. The endogenous CAV1 protein levels were

comparable in HEK293T cells with or without ZNRF2 expression (Figure 12A). In

addition, CAV1 levels and TLR4-driven signaling were not significantly different

between control and ZNRF2-depleted RAW264.7 cells (Figure 12B), indicating that

unlike ZNRF1, ZNRF2 does not modulate CAV1 turnover. These data support the

notion that ZNRF1-mediated ubiquitination regulates CAV1 degradation.

ZNRF1 Regulates CAV1 Protein Stability through Polyubiquitination on its lysine 39

The specific E3 ubiquitin ligase responsible for CAV1 ubiquitination has not yet been identified. ZNRF1 is an E3 ubiquitin ligase that promotes AKT ubiquitination and degradation[57]. Thus, we speculated that ZNRF1 might directly ubiquitinate CAV1 and target it for degradation. Examination of whether ZNRF1 associates with CAV1 using reciprocal co-immunoprecipitation revealed a physical interaction between ZNRF1 and CAV1 transiently expressed in HEK293T cells (Figure 13A). In addition, LPS stimulation in macrophages increased the interaction between endogenous ZNRF1 and CAV1 in a time-dependent manner (Figure 13B).

To map the domains responsible for the interaction between CAV1 and ZNRF1, we constructed six truncated forms of CAV1 (Figure 14A) and two ZNRF1 deletion mutants (Figure 14C). Co-IP experiments demonstrated that deletion of the C-terminal membrane attachment domain (C-MAD) in CAV1 (CAV1(Δ136-178)) resulted in loss of CAV1's ability to bind to ZNRF1, whereas two CAV1 mutants (CAV1(ΔNC) and CAV1(Δ151)), lacking their extreme C-terminal region (a.a.151-178), retained this binding capacity (Figure 14B), indicating that CAV1 interacts with ZNRF1 via its C-MAD domain (a.a. 135-150). Deletion of the N-terminal domain (a.a.1-142) in ZNRF1 (ZNRF1(ΔN142)) led to the loss of its ability to bind to CAV1 (Figure 14D),

43

suggesting that ZNRF1 interacts with CAV1 via its N-terminal domain.

To evaluate if ZNRF1 directly catalyzes CAV1 ubiquitination, we co-transfected

HEK293 cells with either wild-type ZNRF1 or ZNRF1 (C184A) mutant, along with

HA-tagged ubiquitin and determined the level of CAV1 ubiquitination. As expected, a

significant increase in ubiquitinated CAV1 was detected in ZNRF1-overexpressing cells

compared to cells transfected with vector control or the enzymatically inactive mutant

ZNRF1 (C184A) (Supplementary Figure 1A). To examine whether ZNRF1 directly

ubiquitinates CAV1, we reconstituted purified recombinant His-tagged wild-type or

mutant ZNRF1, CAV1 proteins, and other ubiquitination components, and carried out

an *in vitro* ubiquitination assay. We observed CAV1 ubiquitination occurring only when

wild type ZNRF1, but not the ligase inactive C184A mutant, was present

(Supplementary Figure 1B). Investigation of the effect of ZNRF1 deficiency on

ubiquitination of CAV1 in macrophages after treatment with LPS illustrated that LPS

increased CAV1 ubiquitination in wild-type macrophages but had no significant effect

on CAV1 ubiquitination in *Znrf1*$^{\Delta}$ BMDMs (Supplementary Figure 1C). These results

demonstrate that TLR4 activation triggers ZNRF1-dependent CAV1 ubiquitination.

Ubiquitination is a post-translational modification in which ubiquitin is covalently

conjugated to a lysine residue on a target protein. The CAV1 protein contains 12 lysine

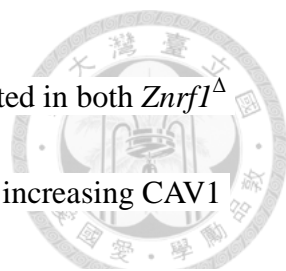residues (Supplementary Figure 2A), many of which have been reported to be ubiquitin

44

binding sites[58, 59]. To determine which lysine in CAV1 is the actual interaction site for

ZNRF1-mediated poly-ubiquitination, we systematically generated CAV1 mutants

containing only a single lysine; all other lysine residues were mutated to arginine to

allow conjugation of only one ubiquitin chain to CAV1. A lysine-free CAV1 mutant

(CAV1(0K)) was also created by mutating all 12 lysine residues to arginine. The CAV1

(39K) mutant, in which all lysine residues were mutated to arginine except lysine 39,

exhibited a ubiquitination pattern similar to that of wild-type CAV1 when co-transfected

with wild-type ZNRF1 into HEK293T cells (Supplementary Figure 2B). To further

confirm that lysine 39 of CAV1 is critical for ZNRF1-mediated ubiquitination, we

substituted lysine 39 of CAV1 with arginine (CAV1(K39R)). CAV1 (K39R) conferred

resistance to ZNRF1-mediated degradation as opposed to wild-type CAV1 when

transiently expressed in HEK293T cells (Figure 15A). In addition, CAV1 (K39R)

expression was associated with a significant decrease in ZNRF1-mediated

poly-ubiquitination (Figure 15B). To determine if ZNRF1-mediated CAV1

ubiquitination is involved in LPS-induced cytokine production, we reconstituted $Cav1^{-/-}$

BMDMs with wild-type CAV1 or CAV1 (K39R) mutant. The reconstitution

of $Cav1^{-/-}$ BMDMs with CAV1 (K39R) was associated with less induction

of TNF, IL-1β and IL-6 mRNA but greater production of IL-10 mRNA compared   to

wild-type CAV1 in response to LPS exposure (Figure 15C). Corresponding to mRNA

45

expression, production of TNF and IL-6 was decreased while IL-10 was enhanced after

TLR4 activation in cells reconstituted with CAV1 (K39R) (Figure 15D).

ZNRF1 Mediates Akt-GSK3β Signalling and Regulates Cytokine Production after stimulation of LPS

It was shown that CAV1 over-expression enhanced Akt activity, leading to

decreased activation of the downstream kinase GSK3β via phosphorylation at serine 9[42].

The suppression of GSK3β was reported to decrease the production of

pro-inflammatory cytokines and increase IL-10 expression in LPS-stimulated immune

cells[44, 45]. Therefore, we examined whether the Akt-GSK3β signaling pathway is

responsible for the dysregulated production of LPS-induced pro-inflammatory and

anti-inflammatory cytokines in ZNRF1-deficient BMDMs. After LPS stimulation,

levels of activated Akt1 with phosphorylated serine 473 were enhanced in both

Znrf1$^{\Delta}$ BMDMs and CAV1-overexpressing RAW264.7 macrophages (Figure 16A). The

protein phosphatase 2A (PP2A), a known dephosphorylation enzyme for Akt, was

previously reported to be blocked by CAV1[60]. To determine whether increased Akt

activation in LPS-treated ZNRF1-depleted cells was due to decreased PP2A activity, we

monitored PP2A activity in both *shZnrf1* and *shScr* cells. PP2A phosphatase activity

was indeed impaired in ZNRF1-depleted cells upon TLR4 engagement (Figure 16B).

46

The inactive form of GSK3β with phosphorylated serine 9 was elevated in both $Znrf1^\Delta$

BMDMs and CAV1-overexpressing RAW264.7 cells, indicating that increasing CAV1

expression suppresses GSK3β activity by enhancing Akt induction in TLR4-activated

macrophages (Figure 17A). GSK3β phosphorylates the transcription factor CREB at

serine 129, resulting in a loss of CREB's DNA-binding capacity[61, 62]. CREB was shown

to be a critical positive regulator of IL-10 transcription, and its activity was enhanced by

inhibiting GSK3β thereby promoting IL-10 mRNA expression[63]. Thus, we assessed

whether Akt-GSK3β signaling upregulated LPS-triggered IL-10 production through

CREB activation in $Znrf1^\Delta$ BMDMs. Indeed, we observed that phosphorylation of

CREB at serine 129 was reduced in $Znrf1^\Delta$ BMDMs and CAV1-overexpressing

RAW264.7 macrophages after LPS stimulation, indicating an increase in CREB

trans-activational activity (Figure 17B). It has been demonstrated that GSK3β

negatively regulates NF-κB activation by inhibiting p65 nuclear translocation[49, 50].

Therefore, the blunted cytokine production in LPS-treated ZNRF1-deficient cells may

have been due to reduced nuclear translocation of NF-κB via the Akt-GSK3β signaling

pathway. As expected, nuclear translocation of NF-κB subunit p65 was markedly

decreased in both $Znrf1^\Delta$ BMDMs and CAV1-upregulated RAW264.7 macrophages

compared to control macrophages (Figure 18). However, there was minimal reduction in

TLR4-activated c-Jun nuclear localization. These data collectively demonstrate that

47

ZNRF1 modulates the production of TLR4-induced pro- and anti-inflammatory

cytokines through the regulation of CAV1 expression and the Akt-GSK3β signaling

pathway.

ZNRF1 Modulates TLR4- and CLP-triggered Inflammatory Responses through the control of CAV1 protein turnover

To further confirm that ZNRF1 mediated TLR4 signaling and cytokine production

through CAV1, we depleted CAV1 expression by siRNA in both $Znrf1^{F/F}$ and

$Znrf1^{\Delta}$ BMDMs. When CAV1 was downregulated in $Znrf1^{\Delta}$ BMDMs, The induction of

$Il10$ and inhibition of $Il1b$, $Il6$ and Tnf expression that normally accompany TLR4

activation had largely disappeared, as compared to control (negative control (NC)) with

CAV1 siRNA (Figure 19A). Accordingly, $Znrf1^{\Delta}$ BMDMs with CAV1 depletion had less

IL-10, but higher pro-inflammatory cytokine production in response to LPS (Figure

19B). Moreover, phosphorylation of Akt1 at Ser 473 and GSK3β at Ser 9 were severely

reduced while CREB phosphorylation at Ser 129 was elevated in LPS-activated $Znrf1^{\Delta}$

BMDMs transfected with CAV1 siRNA, but not in controls with siRNA (Figure 20A).

To confirm the physiological effect of the ZNRF1-CAV1 axis in modulating

inflammatory responses *in vivo*, we systemically depleted CAV1 in $Znrf1^{F/F}$ and $Znrf1^{\Delta}$

mice by intravenous administration of siRNA. Consistent with the result in BMDMs,

48

depletion of CAV1 in *Znrf1*$^{\Delta}$ mice substantially increased plasma IL-6 and TNF, and

decreased IL-10 levels after CLP challenge (Figure 20B). Hence, ZNRF1 regulated

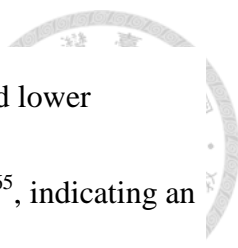TLR4-triggered Akt-GSK3β signaling and inflammation by controlling CAV1 levels.
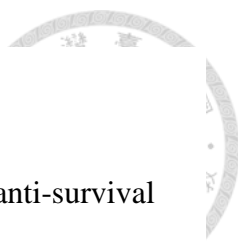
Discussion

The Inflammatory response is promptly induced by the innate immune system upon infection in order to combat the invading pathogens and this process should be controlled rigorously[64]. TLR4 plays a central role in the recognition of LPS from the invading bacteria[9]. Despite extensive investigation, understanding of the regulation of TLR4-mediated inflammatory responses remains fragmented. In this study, we have identified that an E3 ubiquitin ligase, ZNRF1, modulates ubiquitination of CAV1 to regulate TLR4-activated immune responses *in vitro* and *in vivo*. ZNRF1 deficiency resulted in decreased CAV1 ubiquitination and protein turnover, which subsequently inhibited TLR4-initiated inflammatory responses. Mechanistically, ZNRF1-modulated CAV1 expression regulates Akt-GSK3β signaling, whose downstream targets inhibit inflammatory responses by suppressing the induction of pro-inflammatory cytokines and enhancing IL-10 production. Our findings thus demonstrate that ZNRF1 is a novel regulator of TLR4-induced inflammation by controlling CAV1 protein levels.

CAV1 is a major protein component of the lipid rafts on cell membranes known as caveolae. CAV1 plays a role in various biological processes, including membrane receptor trafficking, lipid transport, and tumor growth and migration[52, 53]. The functional roles of CAV1 in innate immunity and inflammation remain controversial and appear to depend on cell type. The depletion of CAV1 in murine macrophages leads to higher

50

production of pro-inflammatory cytokines including TNF and IL-6, and lower

expression of the anti-inflammatory cytokine IL-10 upon LPS challenge[65], indicating an

anti-inflammatory effect for CAV1. However, CAV1-null mice are more resistant to

LPS challenge due to a reduction in lung inflammation[55, 57]. These findings have been

ascribed to the direct or indirect downregulation of TLR4-induced NF-κB activation by

CAV1 deletion[65, 66], implying that CAV1 positively regulates TLR4 signaling in

pulmonary endothelial cells. Nevertheless, recent studies have demonstrated that *Cav1*^{-/-}

mice are more susceptible to infection by various pathogenic bacteria or to CLP

challenge[58, 59] due to an enhanced inflammatory response, revealing a protective role of

CAV1 in bacteria-induced sepsis. Since myeloid cells, including macrophages, are

predominately responsible for cytokine production during sepsis[44], the function of

myeloid CAV1 during sepsis remains elusive. Thus, myeloid cell-specific

CAV1-deficient mice represent a pertinent solution for this issue. Our results show that

ZNRF1 negatively modulates CAV1 protein expression. Both ZNRF1-deficient and

CAV1-overexpressing macrophages exhibited decreased LPS-induced pro-inflammatory

cytokine expression but augmented IL-10 induction in our and other studies[55, 60]; this

phenotype vanished when CAV1 was further knocked down in ZNRF1-deficient cells.

Furthermore, we demonstrated that myeloid cell-specific ZNRF1 deletion protects mice

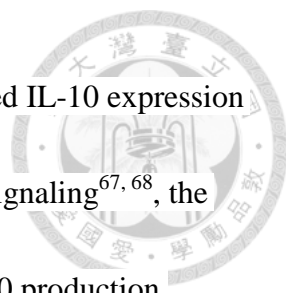from both LPS- and CLP-induced septic death, and depletion of CAV1 reverses the

51

attenuated inflammatory response in $Znrf1^{\triangle}$ mice after CLP, indicating a

pro-inflammatory function for ZNRF1. Our results also suggest that the anti-survival

effect of CAV1 in bacterial- and CLP-induced sepsis is most likely dependent on its

dysregulation of cytokine production in myeloid cells.

Our data reveal that ZNRF1 controls CAV1 protein expression via an

ubiquitin-dependent degradation mechanism, and doesn't share this function with its

closest family member, ZNRF2. Although ubiquitination is crucial for maintaining

CAV1 protein levels, an endolysosome mediated pathway is also involved[38, 39, 61].

However, no E3 ubiquitin ligases responsible for CAV1 ubiquitination have yet been

characterized. To our knowledge, this is the first report describing an E3 ubiquitin ligase

that regulates CAV1 protein ubiquitination and degradation.

ZNRF1 was recently shown to target and degrade Akt through the

ubiquitin–proteasome system in neuronal cells[57]. However, we observed no change in

Akt protein levels but instead hyper-phosphorylation of Akt1 in $Znrf1^{\Delta}$ BMDMs after

TLR4 activation. Our findings demonstrate that in $Znrf1^{\Delta}$ BMDMs, TLR4 activation

causes elevated phosphorylation of Akt, followed by GSK3β inactivation, eventually

resulting in reduced NF-κB nuclear translocation and enhanced CREB transcription. A

similar effect was observed in CAV1-overexpressing RAW264.7 macrophages after LPS

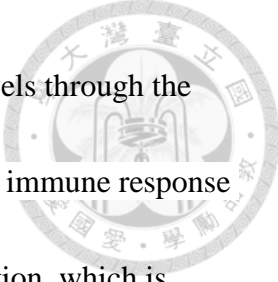stimulation, suggesting a new regulatory role for ZNRF1-CAV1 signaling in

52

TLR4-induced immune responses. Despite the fact that TLR4-induced IL-10 expression

was previously reported to be dependent on type I interferon-IL-27 signaling[67, 68], the

Akt-GSK3β-CREB pathway is also critical for the regulation of IL-10 production

during TLR4 activation[44, 47]. In addition, Akt was previously shown to suppress GSK3β

induction, leading to impaired NF-κB activation[69]. Consistent with these published

findings, elevated CREB activation and attenuated NF-κB p65 nuclear translocation

were observed in LPS-challenged ZNRF1-deficient and CAV1-expressing macrophages

in the present work, suggesting that ZNRF1-CAV1 mainly functions to

regulate Akt-GSK3β-CREB/p65 signaling. It had also been reported that

the over-expression of CAV1 suppresses p65 acetylation, thereby inhibiting NF-κB

activity[70]. However, we did not detect diminished p65 acetylation in $Znrf1^\Delta$ BMDMs

after LPS challenge. Considering this, we are still unable to exclude the possibility that

ZNRF1 modulates NF-κB activity through other mechanisms to mediate the induction

of pro-inflammatory cytokines.

Our data suggest that upregulation of CAV1 caused by ZNRF1 depletion

augments TLR4-induced Akt activation through inhibition of PP2A phosphatase activity.

Numerous studies previously demonstrated a suppressive effect of CAV1 on PP2A

activity[60, 71, 72]. However, a class IA PI3Kδ had been shown to recruit TLR4 to the

plasma membrane, resulting in Akt activation and TLR4 internalization[73]. We observed

53

no difference in LPS-induced TLR4 internalization between control and

ZNRF1-deficient macrophages. A recent report demonstrated that Rab8a, a small

GTPase, is enriched in the dorsal ruffles of TLR4-activated macrophages, where it

recruits and activates a class IB PI3Kγ[69]. The Rab8a-PI3Kγ complex then activates

downstream Akt, leading to the inhibition of inflammatory responses by attenuating the

production of pro-inflammatory cytokines and enhancing the release of IL-10, without

affecting TLR4 internalization. The effect of Rab8a-PI3Kγ-Akt signaling on

TLR4-mediated immune responses is very similar to that in ZNRF1-deficient

macrophages. Thus, we cannot exclude the possibility that ZNRF1-CAV1 signaling

regulates TLR4-induced inflammatory responses through the modulation of PI3Kγ

recruitment and activation, although this hypothesis remains to be verified. In addition,

the upregulation of CAV1 in macrophages appears to affect the TLR4-MyD88 signaling

pathway only. We also observed increased activation of IRF3, which is regulated by

endosomal TLR4-TRIF signaling, in LPS-treated $Znrf1^{\Delta}$ BMDMs. The role of ZNRF1

in endosomal TLR4 signaling and the underlying mechanism await further elucidation.

The activation of macrophages by TLR4 stimulation leads to the production of

several inflammatory mediators, including TNF, IL-1β, and IL-6 that contribute to the

inflammatory response to defend against infections, but also correlates with the severity

of potential sepsis. Our data demonstrate that LPS induces a transient association

between CAV1 and ZNRF1 as well as a decrease in CAV1 protein levels through the

ubiquitin/proteasomal pathway. These effects of LPS allow the innate immune response

to rapidly shift toward pro-inflammatory cytokine/chemokine production, which is

needed to constrain pathogens during the early phase of host infection (Figure 21). LPS

was known to induce CAV1 expression[74]. Hence, CAV1 upregulation might contribute

to the suppression of inflammation at a later phase of infection. CAV1 levels were

reportedly upregulated in senescent cells and animals[71]. Therefore, it may be

worthwhile to investigate age-related defects in innate defenses against pathogen

infection in association with the expression of CAV1 and ZNRF1. In summary, we

determined that ZNRF1 regulates CAV1 turnover and further modulates inflammatory

responses in response to endotoxin, identifying the ZNRF1-CAV1 axis as a new and

non-redundant mechanism for controlling inflammation. We proposed a model

summarizing the control of CAV1 protein level and TLR-triggered immune responses

by ZNRF1 (Figure 21). As excessive CAV1 expression contributes to a variety of

pathological processes in human diseases, including cancer metastasis, atherosclerosis,

and diabetes, our findings may also indicate a novel therapeutic target for the treatment

of these CAV1-related conditions.

Table 1.

Complete blood counts of *Znrf1*$^{\Delta}$ and *Znrf1*$^{F/F}$ mice

Parameters	*Znrf1*$^{F/F}$	*Znrf1*$^{\Delta}$	P-value
RBC (10^6/mm^3)	8.75±0.36	8.82±0.31	0.78
Hb (g/dl)	13.9±0.51	13.8±0.51	0.78
WBC (10^3/mm^3)	2.37±0.86	2.99±0.86	0.22
Lymphocytes (%)	76.61±3.8	77.46±6.83	0.76
Granulocytes (%)	11.68±0.85	12.98±1.89	0.17

These data represent the average values (mean±SD.) for six *Znrf1*$^{\Delta}$ and *Znrf1*$^{F/F}$ mice examined 2 weeks after two poly(I:C) inductions (10 μg/g of body weight on day 0 and day 2).

Table 2.

Primer pairs for RT-qPCR

Mouse *Cyclophilin* Forward:	ATGTGCCAGGGTGGTGACTTT
Mouse *Cyclophilin* Reverse:	TTGCCATCCAGCCATTCAGTC
Mouse *Tnf* Forward:	GTCTACTGAACTTCGGGGTGATC
Mouse *Tnf* Reverse:	TCCACTTGGTGGTTTGCTACG
Mouse *Il6* Forward:	ACAAGAAAGACAAAGCCAGAGTC
Mouse *Il6* Reverse:	ATTGGAAATTGGGGTAGGAAG
Mouse *Il10* Forward:	TGGGTTGCCAAGCCTTATCGG
Mouse *Il10* Reverse:	ACCTGCTCCACTGCCTTGCTC
Mouse *Il1b* Forward:	GAACTCAACTGTGAAATGCCACC
Mouse *Il1b* Reverse:	CCACAGCCACAATGAGTGATACT
Mouse *Ccl5* Forward:	GACACCACTCCCTGCTGCTTTG
Mouse *Ccl5* Reverse:	GATGTATTCTTGAACCCACTTCTT
Mouse *Ifnb* Forward:	GCTGCGTTCCTGCTGTGCTTCT
Mouse *Ifnb* Reverse:	CGCCCTGTAGGTGAGGTTGATC
Human *CYCLOPHILIN* Forward:	ATACGGGTCCTGGCATCTTGTC
Human *CYCLOPHILIN* Reverse:	GGTGATCTTCTTGCTGGTCTTG
Human *TNF* Forward:	CCTGCTGCACTTTGGAGTGATC
Human *TNF* Reverse:	ACTCGGGGTTCGAGAAGATGAT
Human *IL6* Forward:	TGCTTCCAATCTGGATTCAATG
Human *IL6* Reverse:	GGTTGGGTCAGGGGTGGTTATT
Human *IL10* Forward:	CTGAGAACCAAGACCCAGACAT
Human *IL10* Reverse:	AGGCATTCTTCACCTGCTCCAC
Human *IL1B* Forward:	CGAATCTCCGACCACCACTAC
Human *IL1B* Reverse:	GCACATAAGCCTCGTTATCCC

A

Wild-type allele — Exon 2 — Exon 3 — Exon 4 —

1st targeting vector — ▶ Neo ▶ — Exon 2 —

Transient Cre transfection

— Exon 2 — Exon 3 — Exon 4 —

2nd targeting vector — Exon 3 — ● Neo ● ▶ — Exon 4 —

Targeted allele — ▶ — Exon 2 — Exon 3 — ● Neo ● ▶ — Exon 4 —

Transient Flp transfection

Floxed allele

Probe ◀

— ▶ — Exon 2 — Exon 3 — ● ▶ — Exon 4 —

EcoR1 | — | |

1kb 8kb

Primer_F ◀   ◀ Primer_R

Δ allele — Exon 1 — ▶ — Exon 4 —

▶ Flox
● FRT

B

Znrf1   *Mx1-Cre:Znrf1*

+/+ F/+ F/F (-)   +/+ F/+ F/F

← Floxed band
← Wild type band

← Creband

C

Znrf1$^{F/F}$ *Znrf1*^{Δ}

Kidney Liver Lung   Kidney Liver Lung

← Floxed band

← Cre band

Figure 1. Strategy for generation of Znrf1 conditional knockout mice

(A) Schematic diagram of the mouse wild-type *Znrf1* allele, the two targeting constructs, *Znrf1*^{Flox}-targeted alleles, and the deleted (Δ) *Znrf1* allele after *Cre*-mediated recombination. The initial targeting of the *Znrf1* allele created a new EcoRI restriction site in the first intron. The new EcoRI site resulted in a smaller EcoRI-digested fragment in Southern blot analysis. Arrowheads indicate the positions of the two primers used for PCR genotyping. (B and C) Genotyping of *Znrf1* alleles and *Cre* transgene by PCR using genomic DNA isolated from mouse (B) tails and (C) kidneys, livers, and lungs.
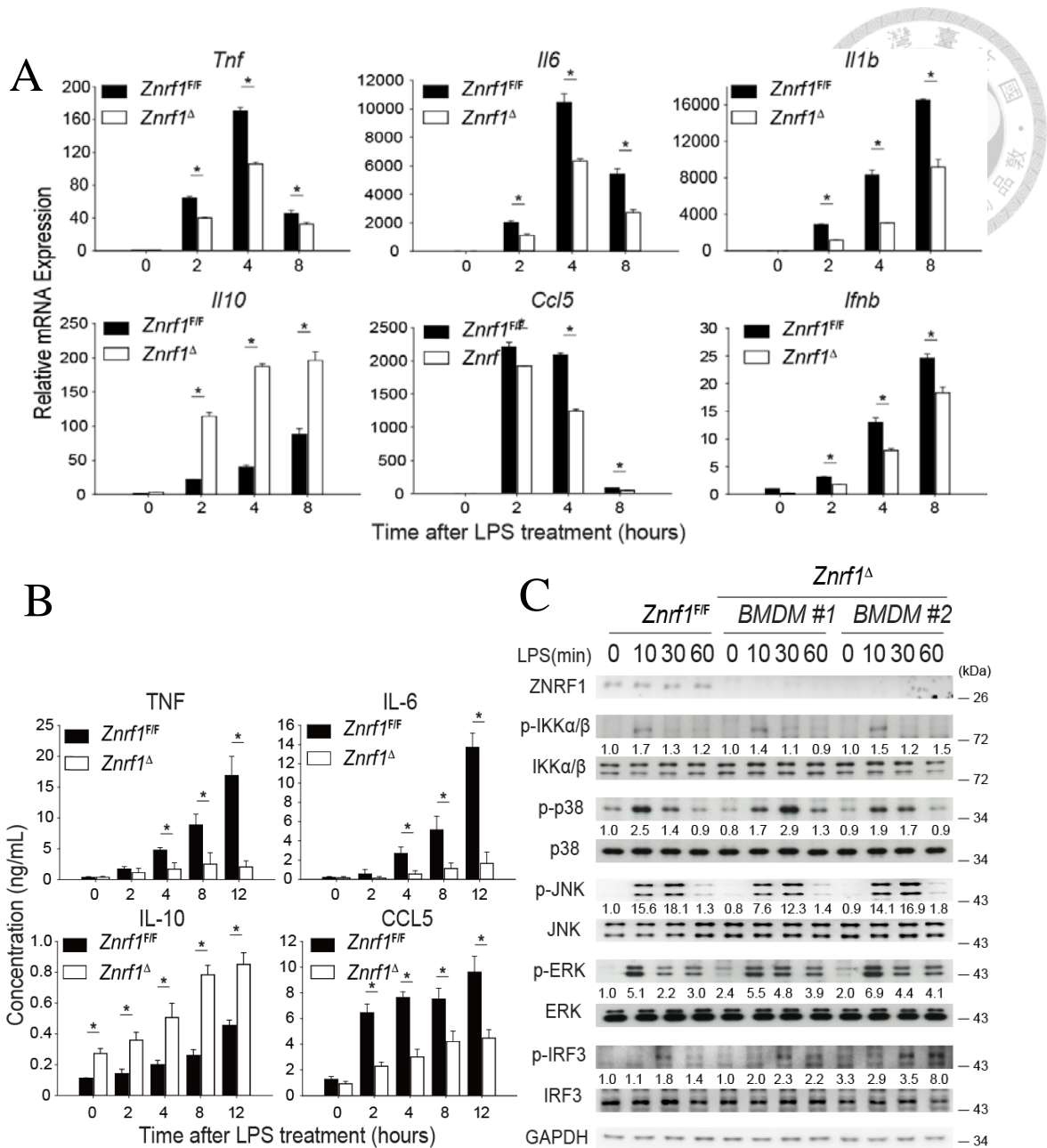
Figure 2. ZNRF1 deficiency impairs pro-inflammatory cytokine production in response to LPS.

(A) BMDMs were harvested from wild-type ($Znrf1^{F/F}$) or $Znrf1^{\Delta}$ mice and treated with LPS (100 ng/ml) for the indicated times. The expression of the indicated mRNAs was analyzed by RT-qPCR. (B) The production of cytokines in supernatants of $Znrf1^{F/F}$ and $Znrf1^{\Delta}$ BMDMs treated with LPS (100 ng/ml) for the indicated times was determined by ELISA. (C) Immunoblot analysis of the phosphorylation of MAPKs, IKKα/β, and IRF3

in lysates of *Znrf1*$^{F/F}$ and *Znrf1*$^{\Delta}$ BMDMs stimulated with LPS (100 ng/ml) for the indicated times. The intensities of the bands are expressed as fold increases compared to those of untreated control cells after normalization to their unphosphorylated forms.

61
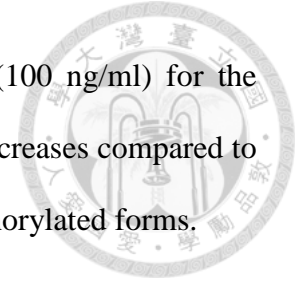
A
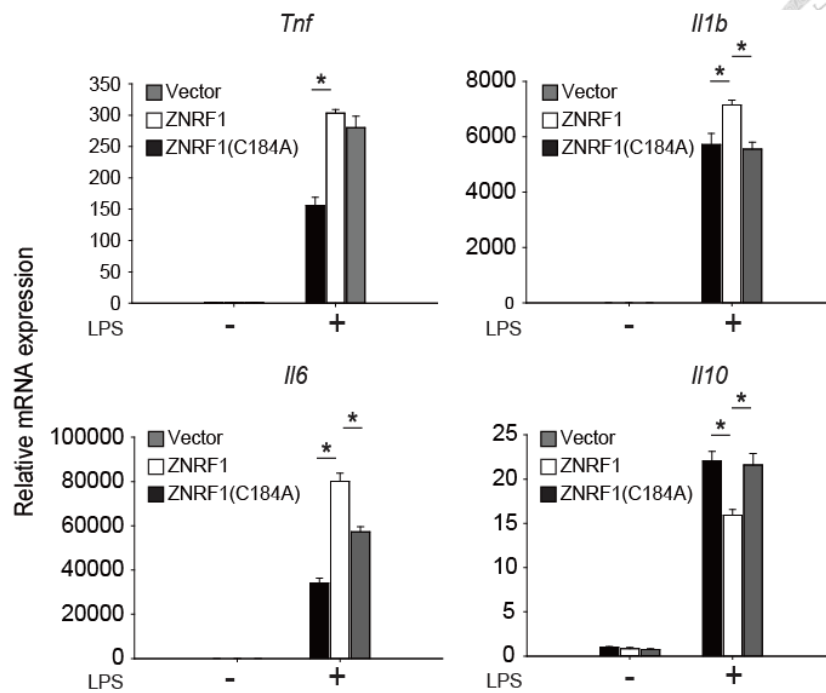
B
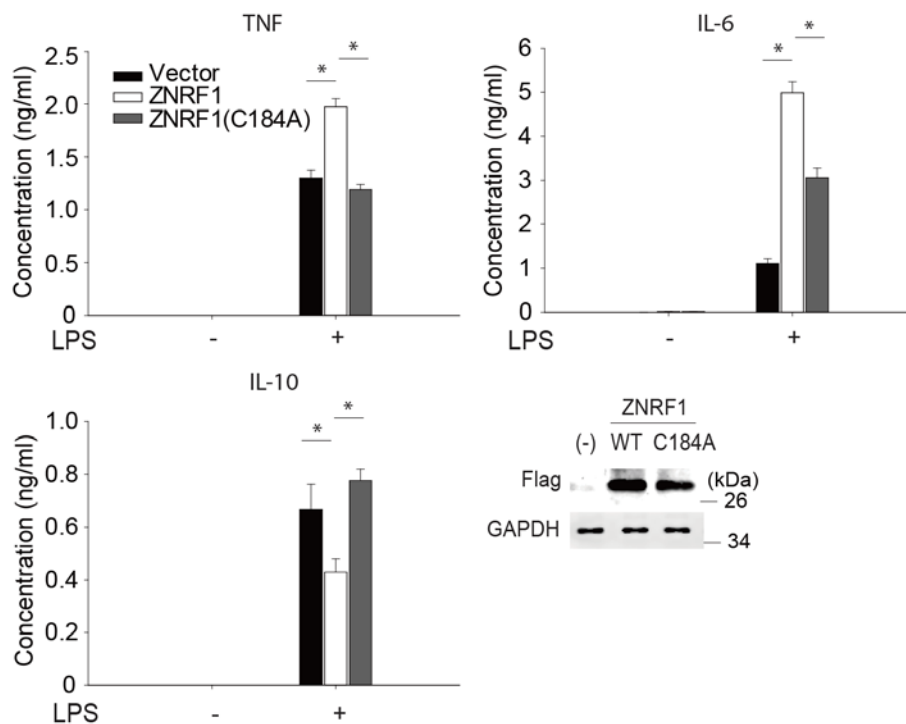
Figure 3. The ubiquitin ligase activity of ZNRF1 is required for its suppressive effect on LPS-induced cytokine production.

(A) BMDMs from $Znrf1^{\Delta}$ mice were reconstituted with either Flag-tagged wild-type ZNRF1 or ZNRF1(C184A) mutant and stimulated with LPS (100 ng/ml) for 4 hours

(*Tnf* and *Il6)* or 8 hhours (*Il1b* and *Il10*). (B) BMDMs from *Znrf1*$^{\Delta}$ mice were reconstituted with either Flag-tagged wild-type ZNRF1 or ZNRF1(C184A) mutant and stimulated with LPS (100 ng/ml) for 10 hours. The levels of the indicated cytokines in culture supernatants were measured by ELISA.The expression of the indicated mRNAs was measured by RT-qPCR. *P<0.05 (Student's *t*-test). These data are representative of three independent experiments performed in triplicate (error bars, SD.).
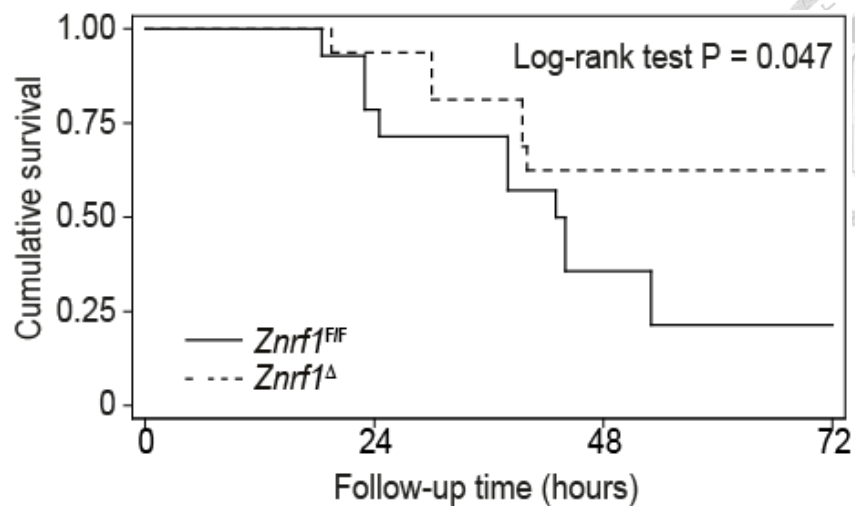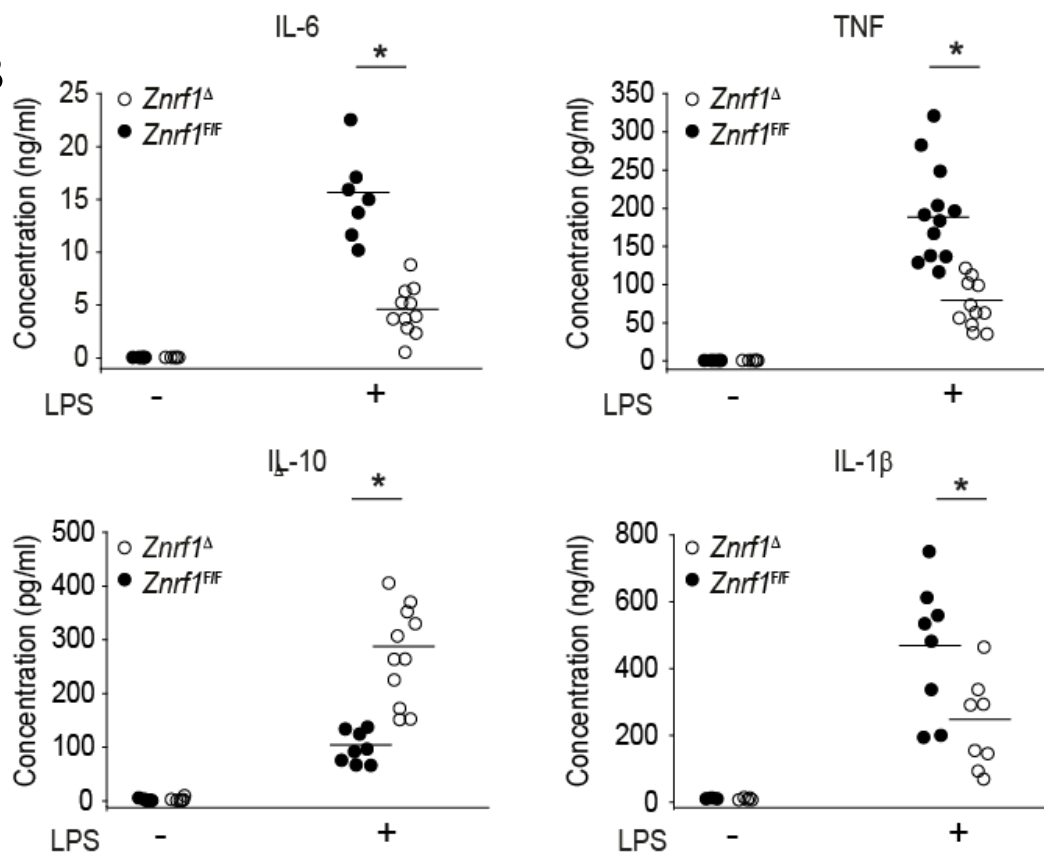
Figure 4. *Znrf1*$^\Delta$ mice are resistant to LPS-induced sepsis.

(A) Survival of *Znrf1*$^\Delta$ (gray line, n=11) and *Znrf1*$^{F/F}$ mice (solid line, n=11) with intraperitoneal injection of LPS (15 mg/kg of body weight). (B) ELISA analysis of the indicated cytokines in sera from *Znrf1*$^\Delta$ and *Znrf1*$^{F/F}$ mice 6 hours after LPS challenge. *P<0.05 (Student's *t*-test). (error bars, SD.).

64
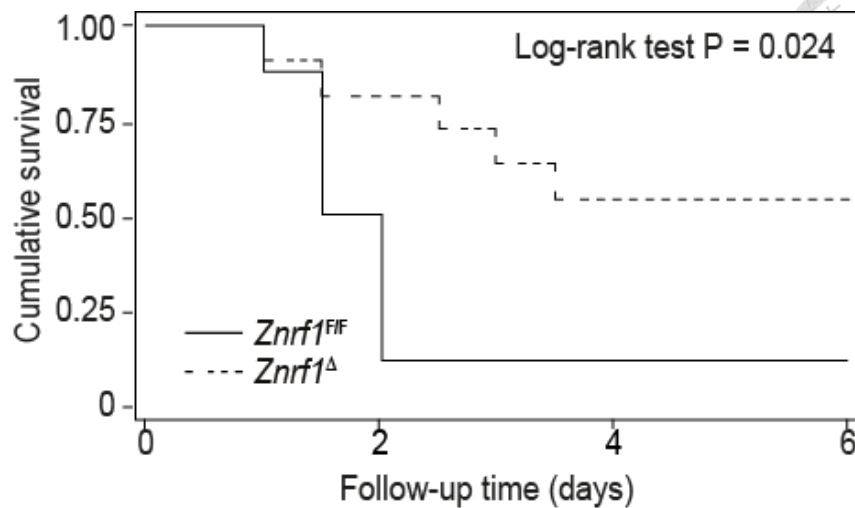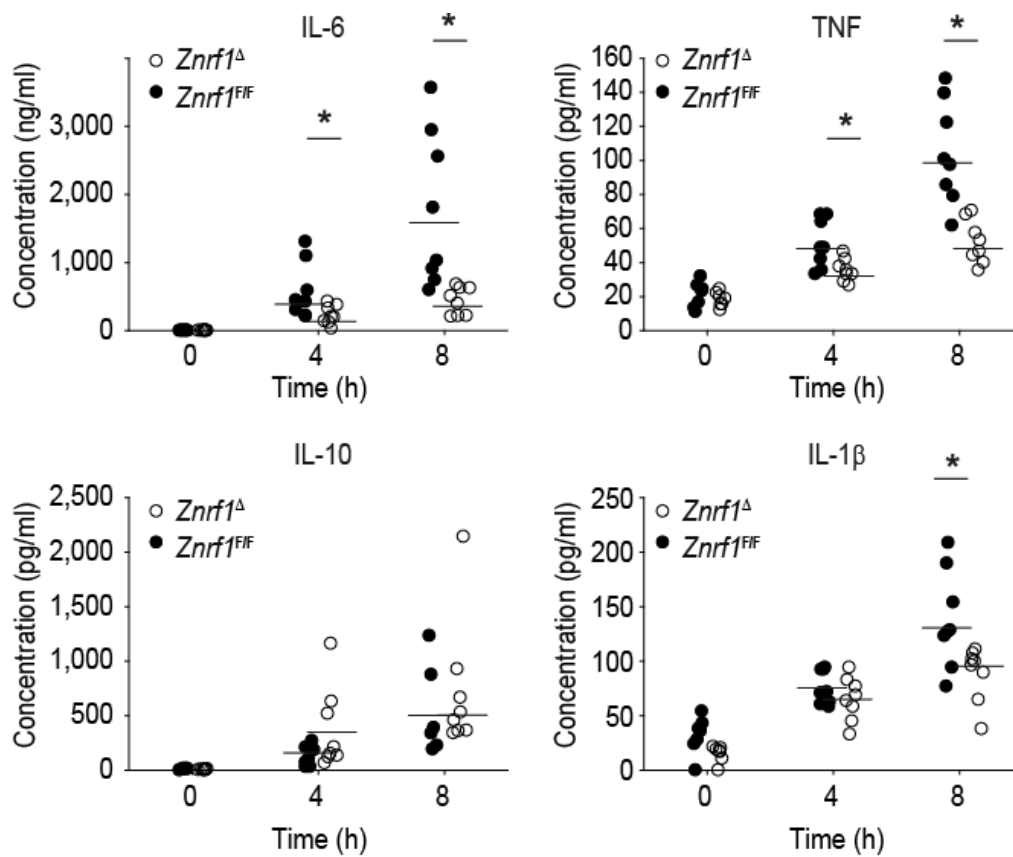
Figure 5. _Znrf1_$^\Delta$ mice are resistant to CLP-induced sepsis.

(A) Survival of _Znrf1_$^\Delta$ mice (dotted line, n=8) and _Znrf1_$^{F/F}$ mice (solid line, n=8) after

CLP challenge. (B) ELISA analysis of the indicated cytokines in sera from _Znrf1_$^\Delta$ and

Znrf1$^{F/F}$ mice collected 0, 4, and 8 hours after the CLP procedure. *P<0.05

(Student's _t_-test). (error bars, SD.).
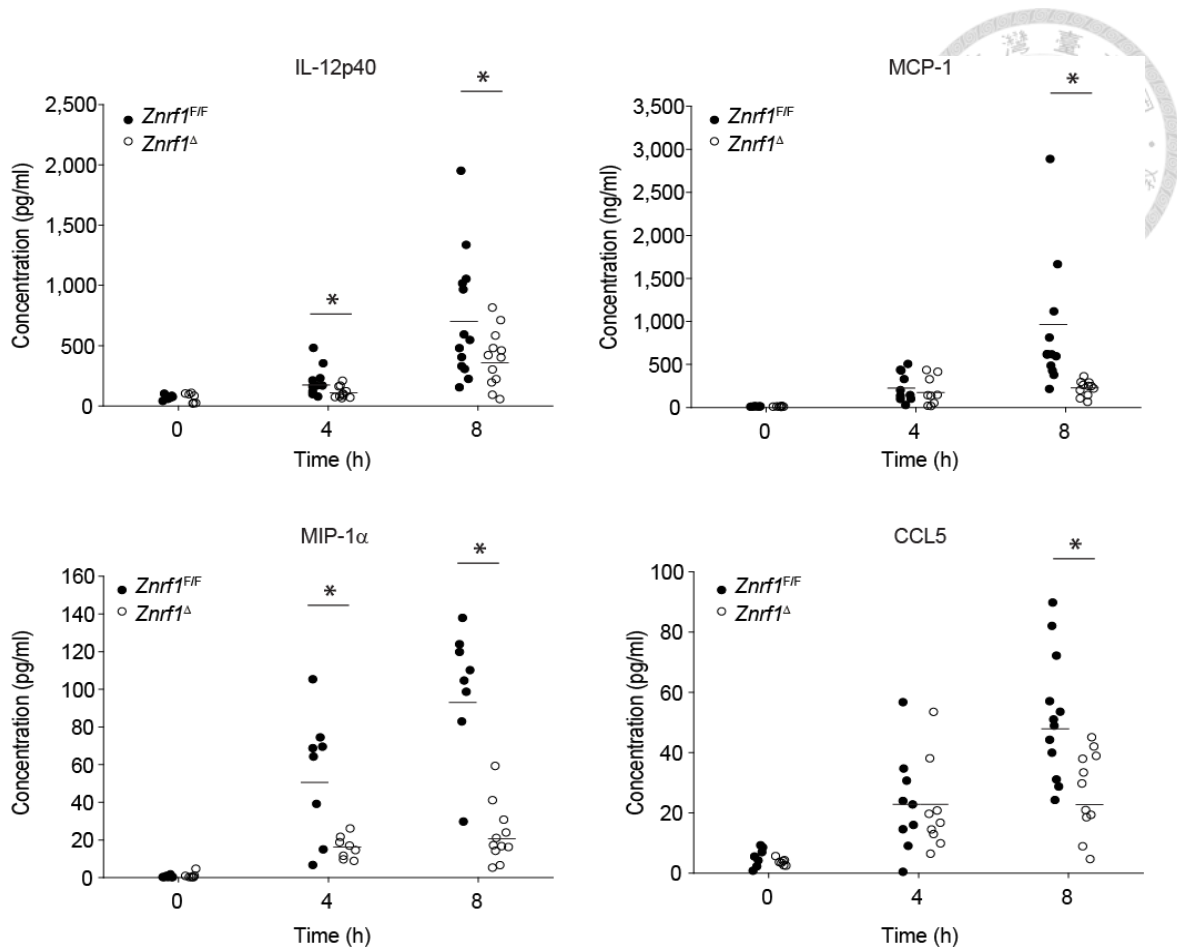
Figure 6. Serum from *Znrf1*$^{\Delta}$ mice possess decreased cytokine and chemokine production after CLP.

Sera were collected from *Znrf1*$^{\Delta}$ and *Znrf1*$^{F/F}$ mice 8 hours after CLP, and the levels of IL12p40, MCP-1, MIP-1α and CCL5 were measured by ELISA. *P<0.05 (Student's *t*-test)
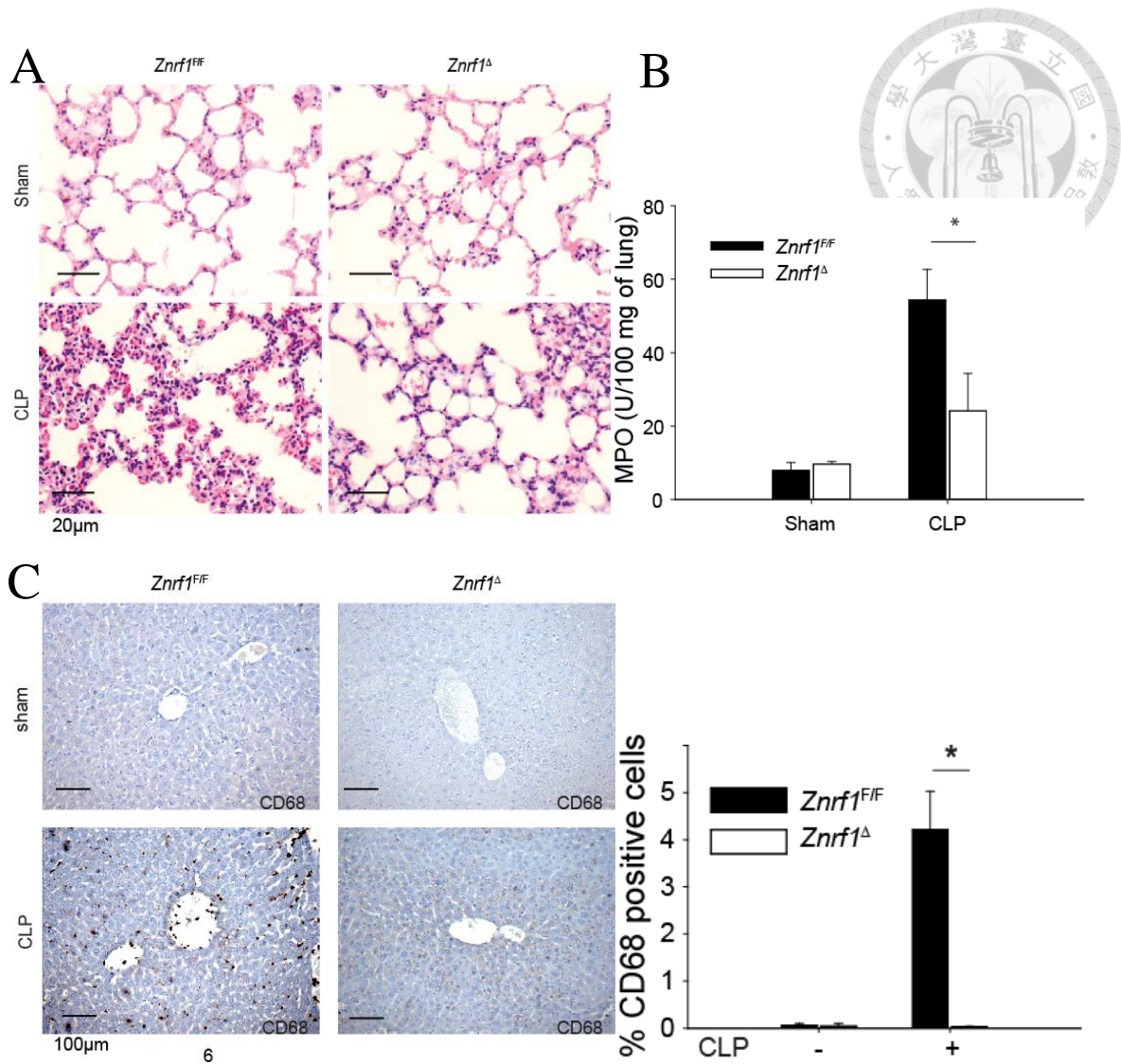
Figure 7. CLP-challenged _Znrf1_$^\Delta$ mice display reduced lung injury.

(A) Hematoxylin and eosin staining of histological sections of lung tissues collected from _Znrf1_$^\Delta$ and _Znrf1_$^{F/F}$ mice (lower panel) 8 hours after CLP and from sham-operated control mice (upper panel). Objective magnification, ×20. Scale bar is 20 μm. (B) The MPO activity in lung tissues from _Znrf1_$^\Delta$ and _Znrf1_$^{F/F}$ mice 8 hours after CLP. *P<0.05 (Student's _t_-test). (error bars, SD.). (C) Liver tissues from _Znrf1_$^\Delta$ and _Znrf1_$^{F/F}$ mice after CLP and sham control (upper panel) were subjected to immunohistochemical staining for CD68 (objective magnification ×20). Scale bar is 100 μm. The total numbers of CD68$^+$ cells per field were quantified and are shown in the lower panel. (Error bars, SD.

from 10 fields of view on 10 sections from lung and liver per mouse, n=4 mice per group). *P<0.05 (Student's *t*-test).
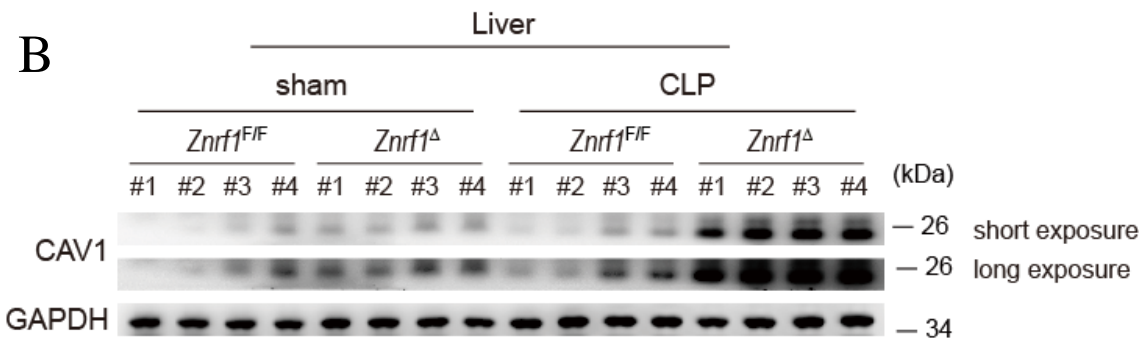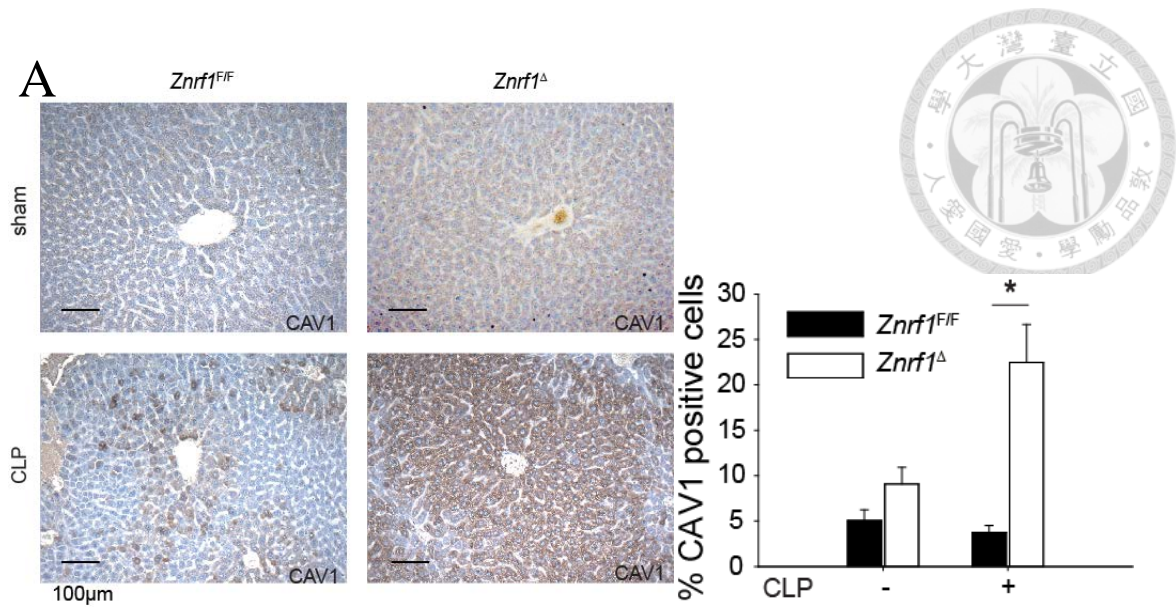
Figure 8. CAV1 protein expression is increased in *Znrf1*$^{\Delta}$ liver.

(A) Liver tissues from *Znrf1*$^{\Delta}$ and *Znrf1*$^{F/F}$ mice (lower panel) 8 hours after CLP and sham control (upper panel) were subjected to immunohistochemical staining for CAV1 (objective magnification ×20). Scale bar is 100 μm. The total numbers of CAV1$^+$ cells per field were quantified and are shown in the lower panel. (Error bars, SD. from 10 fields of view on 10 sections from lung and liver per mouse, n=4 mice per group). *P<0.05 (Student's *t*-test). (B) CAV1 protein levels in liver from *Znrf1*$^{\Delta}$ and *Znrf1*$^{F/F}$ mice 8 hours after CLP or sham operation were examined by western blot. (n=4 mice per group).
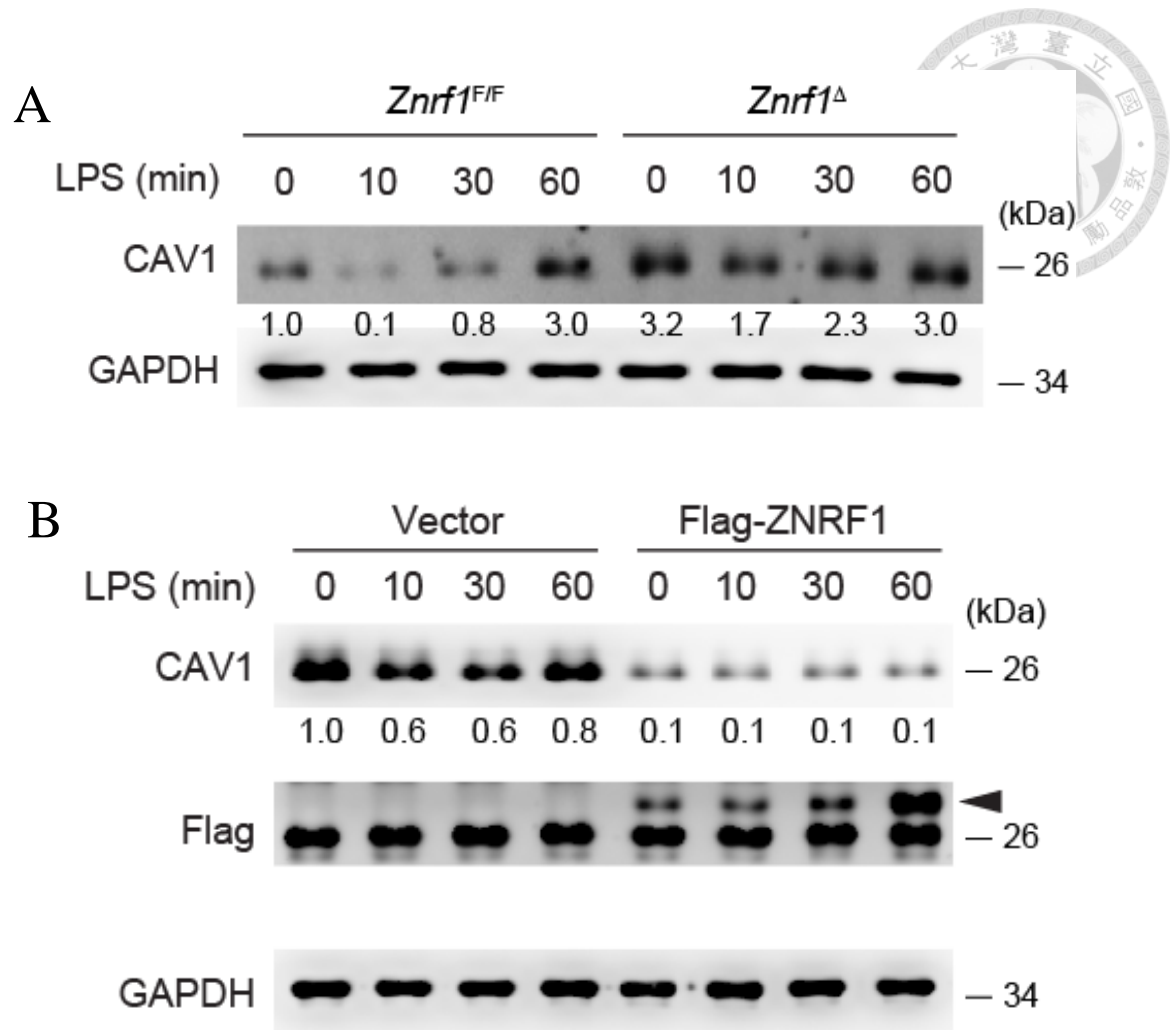
Figure 9. ZNRF1 regulates CAV1 protein expression.

(A) Immunoblot analysis of CAV1 and GAPDH in lysates of $Znrf1^{F/F}$ and $Znrf1^{\Delta}$ cells treated with LPS (100 ng/ml) for the indicated times. (B) Immunoblot analysis of the indicated proteins in lysates of control (vector) and Flag-tagged ZNRF1-expressing RAW264.7 macrophages stimulated with LPS (100 ng/ml). The arrow indicates Flag-ZNRF1.
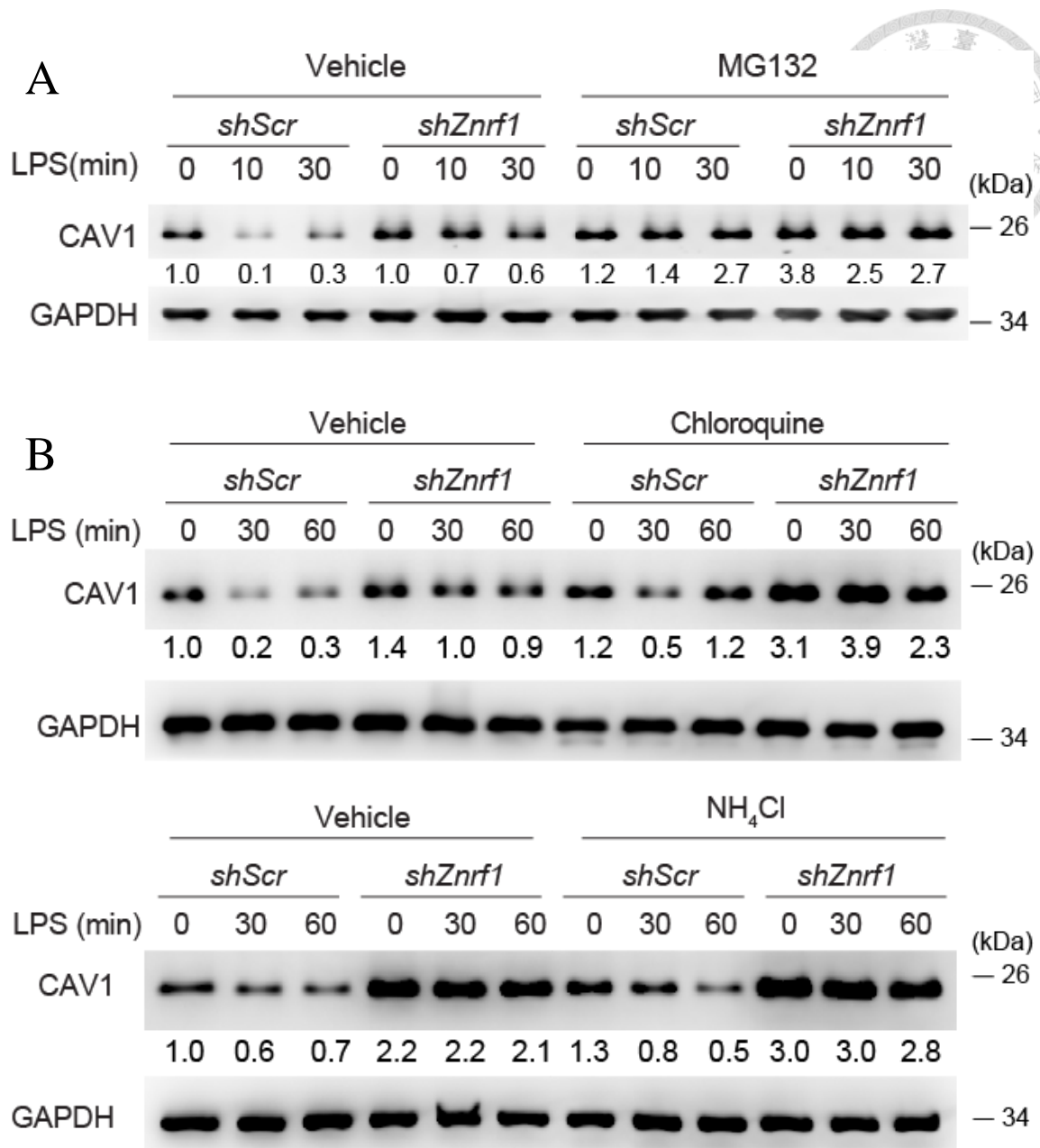
Figure 10. ZNRF1-mediated CAV1 protein degradation is through the proteasome pathway in response to LPS.

(A) Immunoblot analysis of the CAV1 protein in lysates of scrambled control and *Znrf1*-knockdown RAW264.7 cells stimulated with 100 ng/ml LPS with or without pretreatment with MG132 (10 μM). (B) Control and *shZnrf1*-expressing RAW264.7 cells pretreated with chloroquine (100 μM) or NH₄Cl (10 mM) were incubated with LPS (100 ng/ml) for the indicated times. CAV1 protein expression was analyzed by

immunoblotting. The intensities of the bands are shown as fold increases compared to those of untreated control cells after normalization to GAPDH expression. These data are representative of two or three independent experiments performed in triplicate (error bars, SD.).
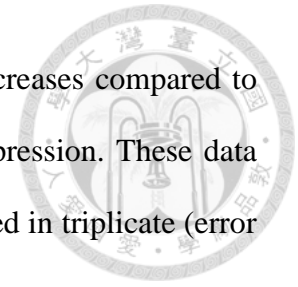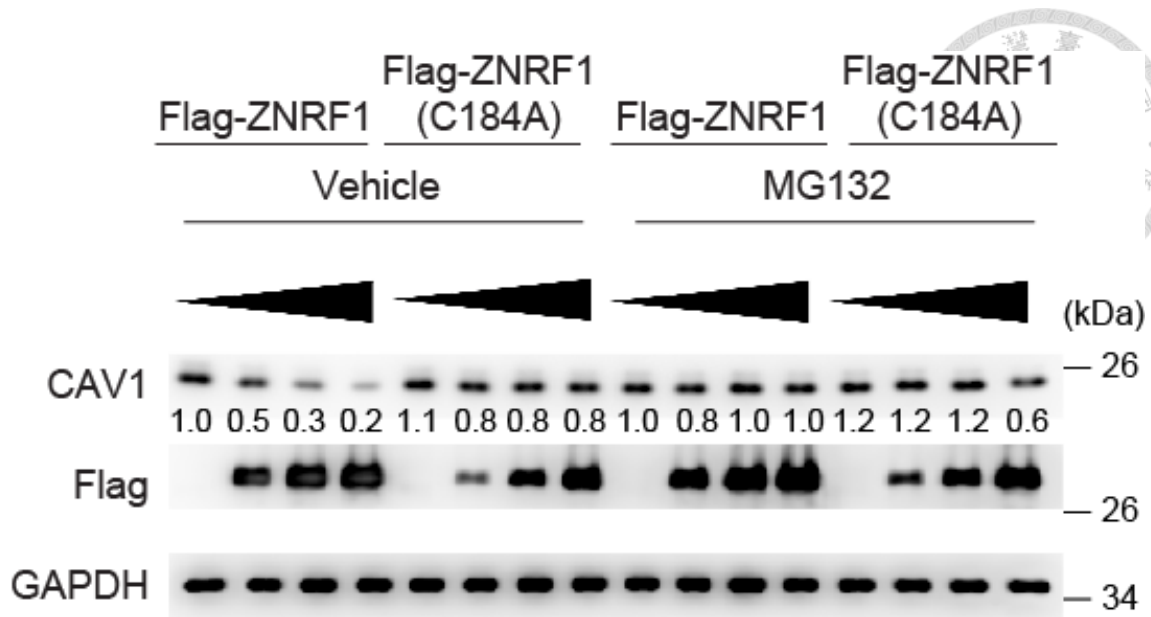
Figure 11. The E3 Ubiquitin activity of ZNRF1 is required for CAV1 degradation.
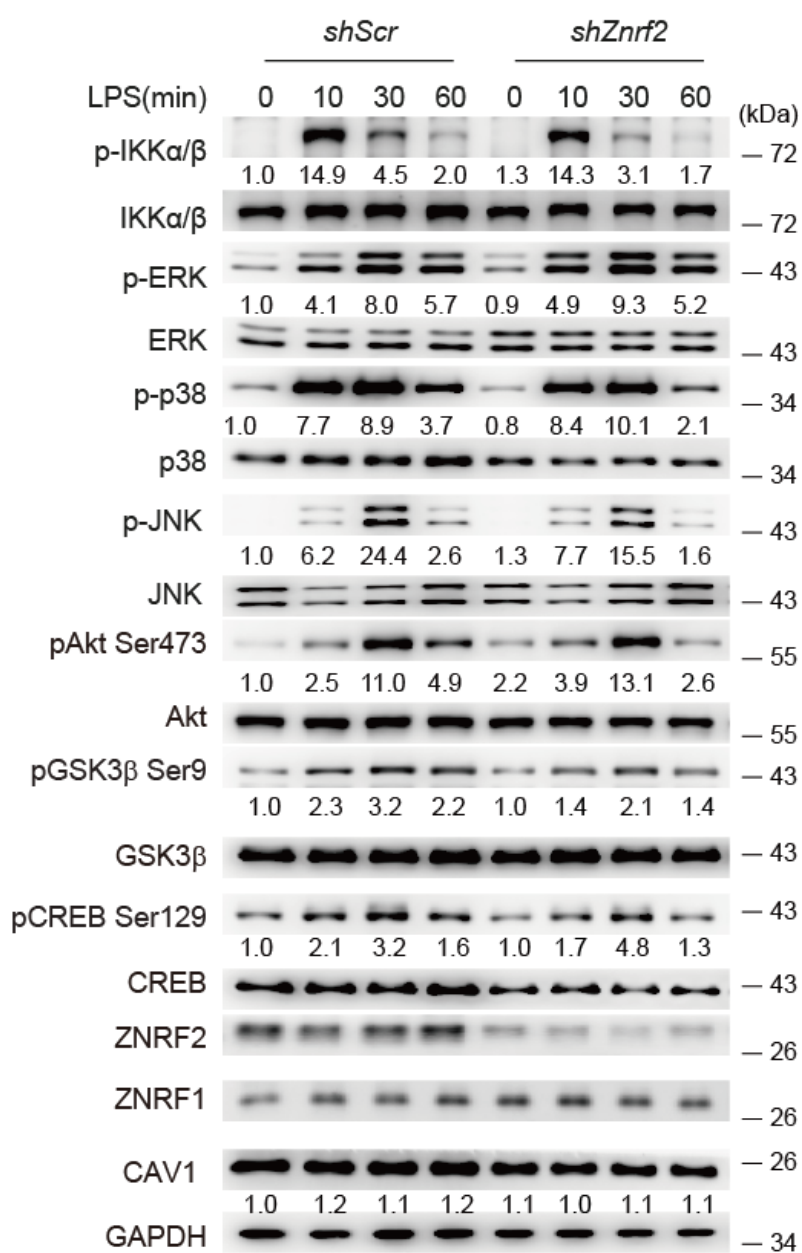
HEK293T cells were transfected with increasing amounts of Flag-tagged wild-type ZNRF1 or ZNRF1(C184A); 24 hours after transfection, the cells were treated with MG132 (10 μM) for at least 6 hours, and cell lysates were analyzed by immunoblotting with the indicated antibodies. The intensities of the bands are expressed as fold increases compared to those of untreated control cells after normalization to GAPDH expression. These data are representative of three independent experiments performed in triplicate.
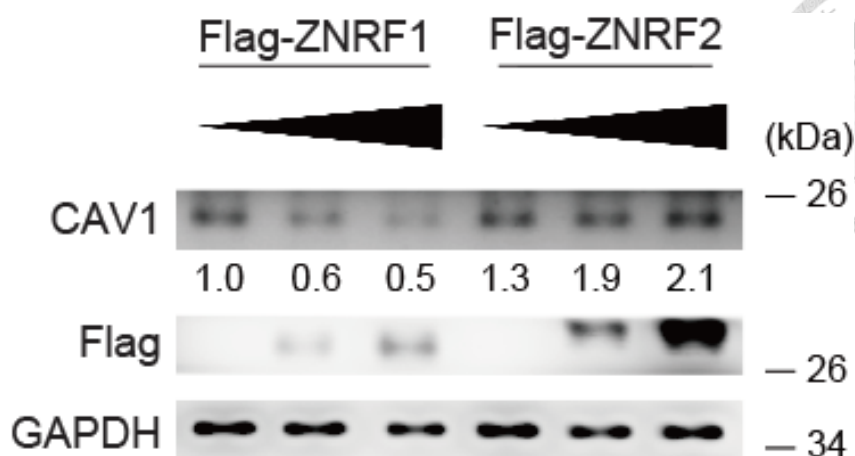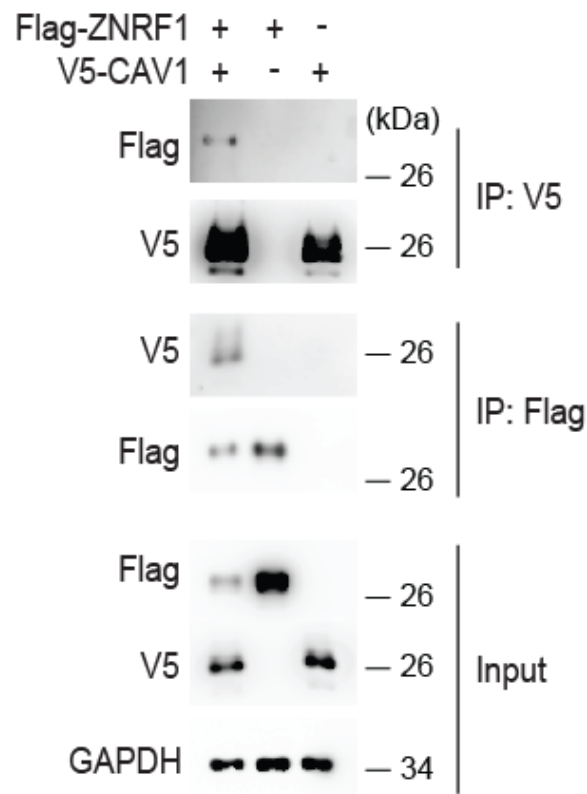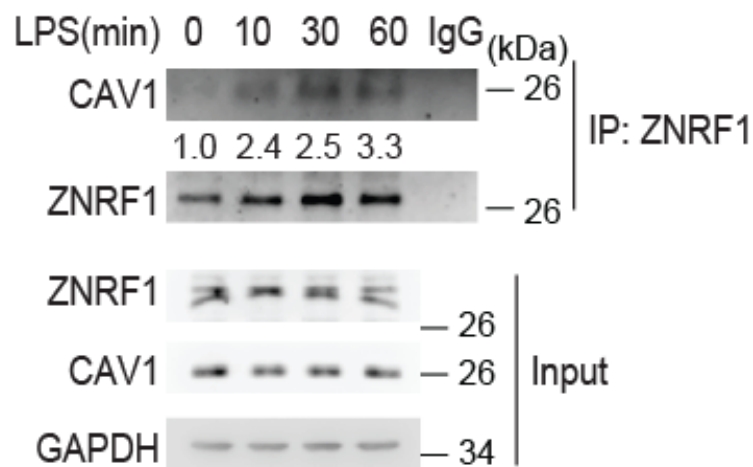
Figure 12. ZNRF2 does not mediate CAV1 protein expression and TLR4 signaling.

HEK293T cells were transfected with increasing amounts of Flag-tagged wild-type ZNRF1 or ZNRF2; 24 hours after transfection, cell lysates were analyzed by immunoblotting with the indicated antibodies. (B) RAW264.7 macrophages infected with lentiviruses expressing *shScr* or *shZnrf2* were stimulated with LPS (100 ng/ml) for the indicated times. Cell lysates were analyzed by immunoblotting with the indicated antibodies. The intensities of the bands are shown as fold increases compared to those of untreated control cells after normalization to their unphosphorylated forms or GAPDH expression. The data are representative of three independent experiments.

75

A

Flag-ZNRF1 + + -
V5-CAV1 + - +

Flag   (kDa)
           — 26   IP: V5
V5   — 26

V5   — 26
                   IP: Flag
Flag   — 26

Flag   — 26
V5   — 26   Input
GAPDH   — 34

B

LPS(min) 0   10   30   60   IgG (kDa)
CAV1   — 26
        1.0 2.4 2.5 3.3   IP: ZNRF1
ZNRF1   — 26

ZNRF1   — 26
CAV1   — 26   Input
GAPDH   — 34

Figure 13. ZNRF1 associates with CAV1

(a) HEK293T cells were co-transfected with V5-tagged CAV1 and Flag-tagged ZNRF1 as indicated. Interactions between ZNRF1 and CAV1 were detected by immunoprecipitation followed by immunoblot analysis with the indicated antibodies. (b) Immunoprecipitation of ZNRF1 from lysates of RAW264.7 cells treated with LPS (100 ng/ml) for the indicated times, followed by immunoblot analysis with the indicated

76

antibodies. The intensities of the bands are shown as fold increases compared to those of untreated cells after normalization to ZNRF1 level. The data are representative of three independent experiments performed in triplicate.
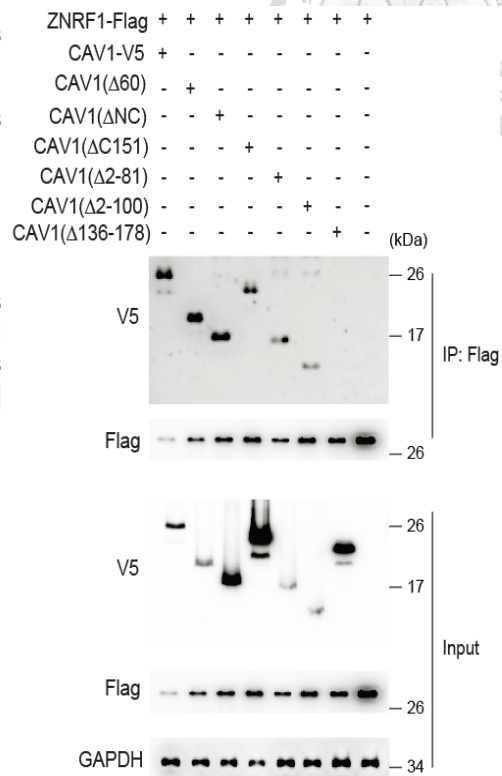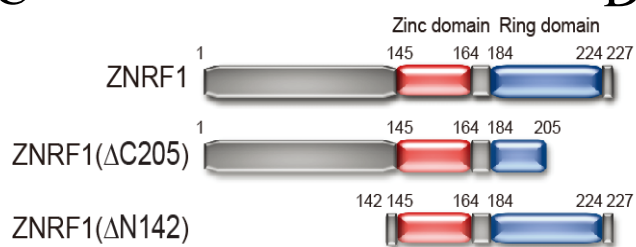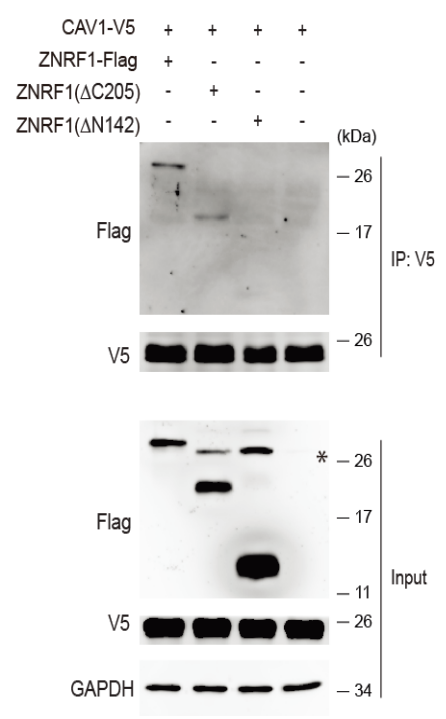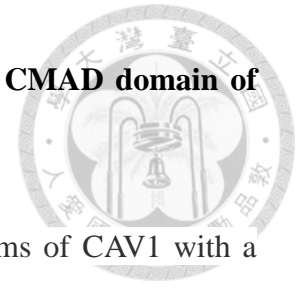
77

doi:10.6342/NTU201700165
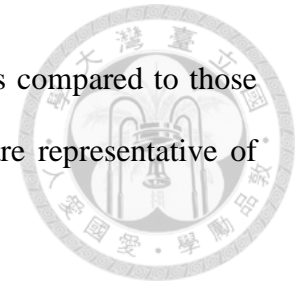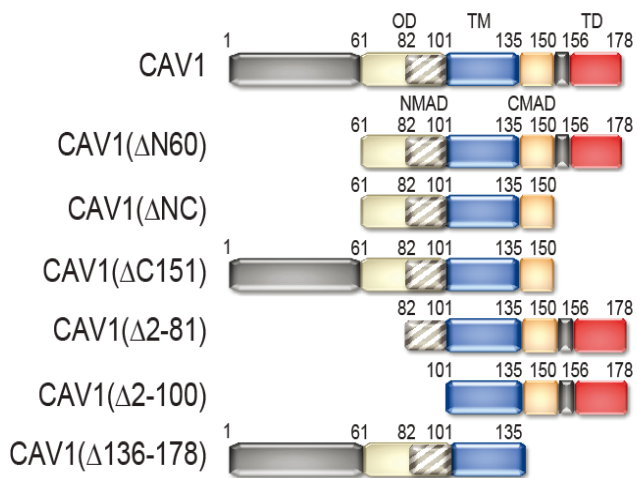
Figure 14. Amino acids 1-145 region of ZNRF1 interacts with CMAD domain of CAV1.

(A) Schematic diagram of full-length CAV1 and six truncated forms of CAV1 with a C-terminal V5 tag. (B) HEK293T cells were co-transfected with Flag-tagged ZNRF1 and V5-tagged full-length or truncated CAV1 as indicated, and interactions between CAV1 and ZNRF1 were identified by immunoprecipitation and immunoblotting with the indicated antibodies. (C) Schematic diagram of full-length ZNRF1 and two truncated forms of ZNRF1 with a C-terminal Flag-tag. (D) HEK293T cells were co-transfected with V5-tagged CAV1 and Flag-tagged full-length or truncated form of ZNRF1 as indicated, and interactions between CAV1 and ZNRF1 were identified by immunoprecipitation and immunoblotting with the indicated antibodies.
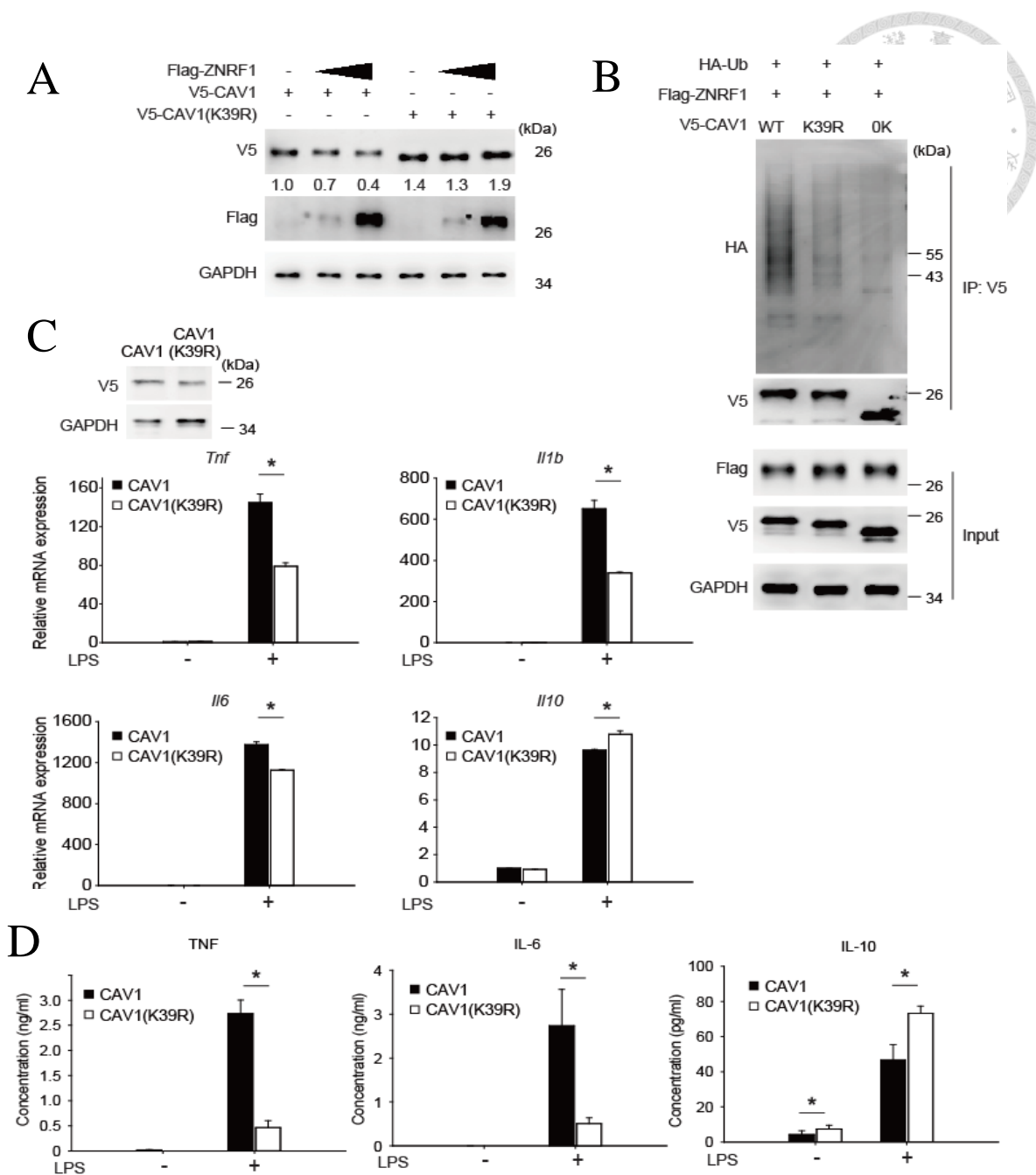
Figure 15. ZNRF1 catalyzes CAV1 ubiquitination at lysine 39 to control its protein turnover and LPS-induced inflammatory cytokine production.
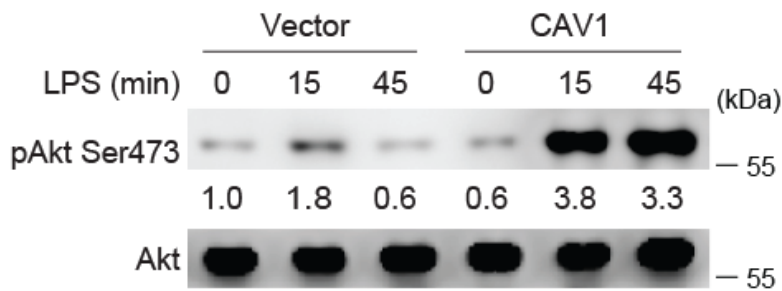
(A) Immunoblot analysis of V5-tagged CAV1 in lysates from HEK293T cells expressing increasing amounts of ZNRF1 and either wild-type CAV1 or the CAV1 (K39R) mutant as indicated. The intensities of the bands are shown as fold increases compared to those of control cells after normalization to GAPDH expression. (B) Immunoprecipitation of V5-tagged CAV1 proteins in lysates from HEK29T cells

expressing Flag-ZNRF1 and either V5-CAV1 or CAV1(K39R), followed by immunoblotting with anti-HA antibody. (C and D) *Cav1*^{-/-} BMDMs were reconstituted with either V5-CAV1 or CAV1 (K39R) and treated with LPS (100 ng/ml). (C) The mRNA expression levels of cytokines at 4 hours post-LPS exposure were analyzed by RT-qPCR, and (D) cytokine levels in supernatants were detected by ELISA at 12 hours after LPS treatment. *$P<0.05$ (Student's *t*-test). These data are representative of three independent experiments performed in triplicate (error bars, SD.).
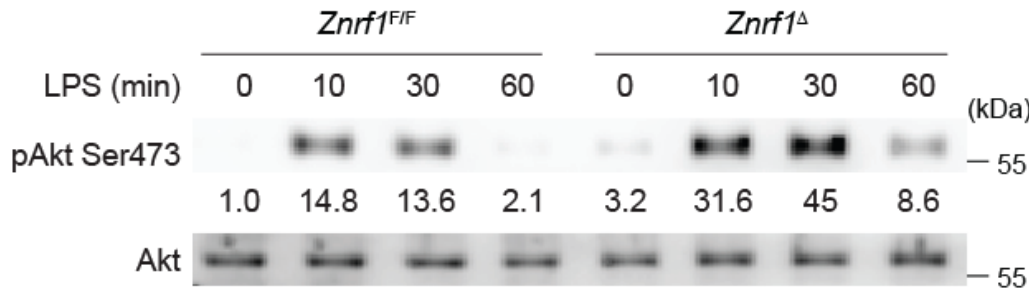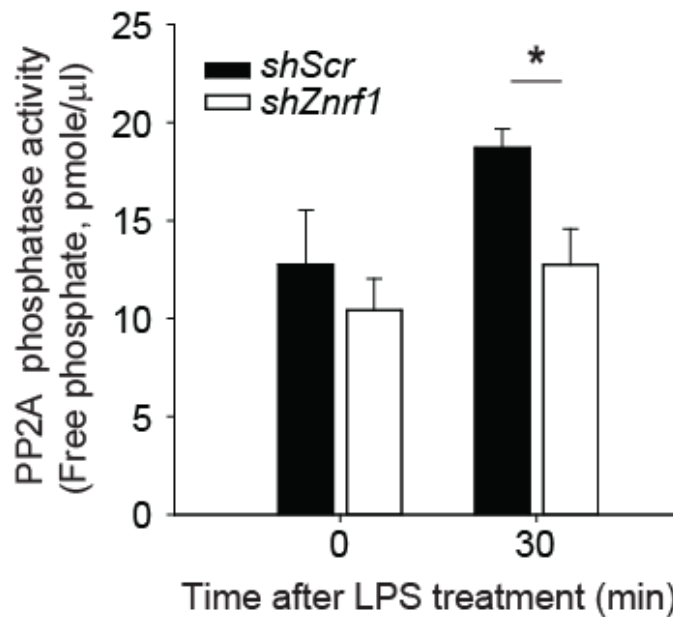
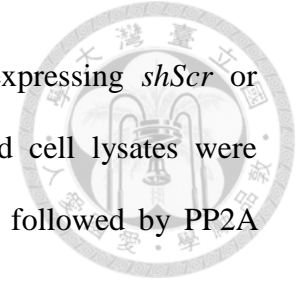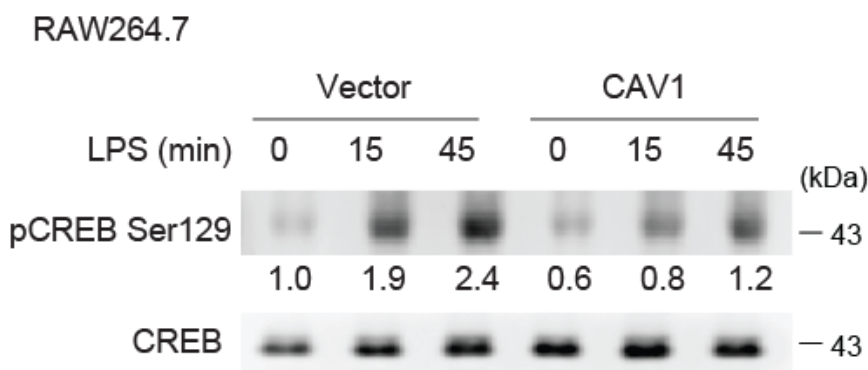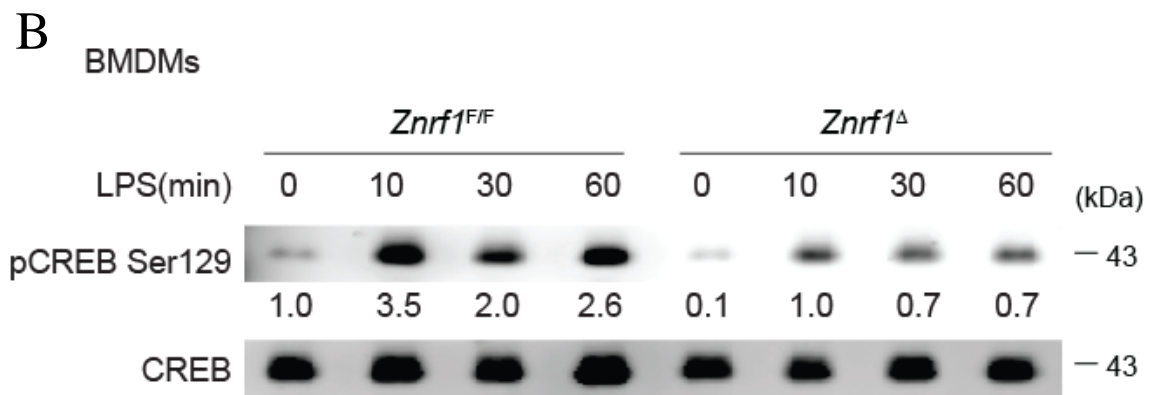**Figure 16. AKT activation is enhanced in ZNRF1-deficient and CAV1-expressing macrophages in response to LPS.**

(A) Immunoblot analysis of the phosphorylation of Akt (Ser473) as well as total Akt, GSK3β, and CREB in lysates of $Znrf1^{F/F}$ and $Znrf1^{\Delta}$ BMDMs and vector- and CAV1-expressing RAW264.7 cells stimulated with LPS (100 ng/ml) for the indicated

times. (B) RAW264.7 macrophages infected with lentiviruses expressing *shScr* or *shZnrf1* were treated with LPS (100 ng/ml) for 30 minutes, and cell lysates were prepared and the PP2A catalytic subunit was immunoprecipitated followed by PP2A phosphatase activity analysis.
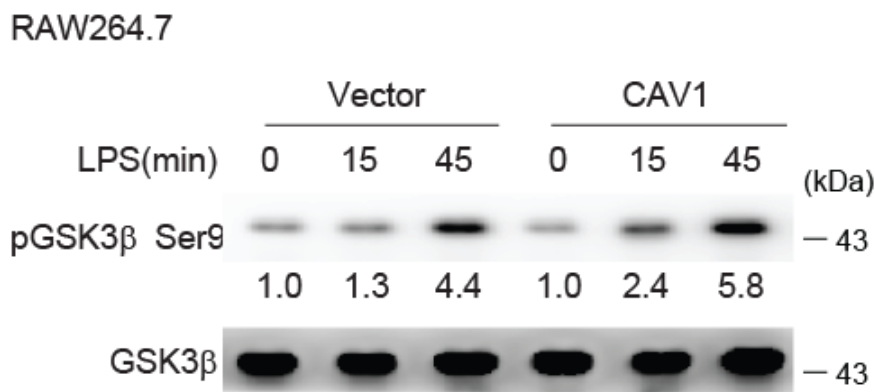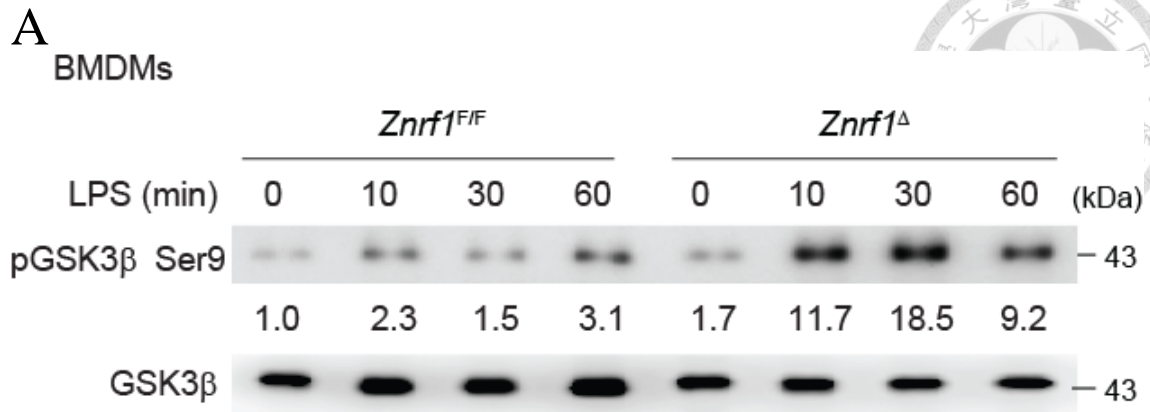
Figure 17. Akt-GSK3β-CREB signaling is altered in ZNRF1-deficient and CAV1-expressing macrophages after LPS stimulation.

(A, B) Immunoblot analysis of the phosphorylation of GSK3β (Ser9) and CREB (Ser129) as well as total GSK3β, and CREB in lysates of *Znrf1*[F/F] and *Znrf1*[Δ] BMDMs and vector- and CAV1-expressing RAW264.7 cells stimulated with LPS (100 ng/ml) for the indicated times.
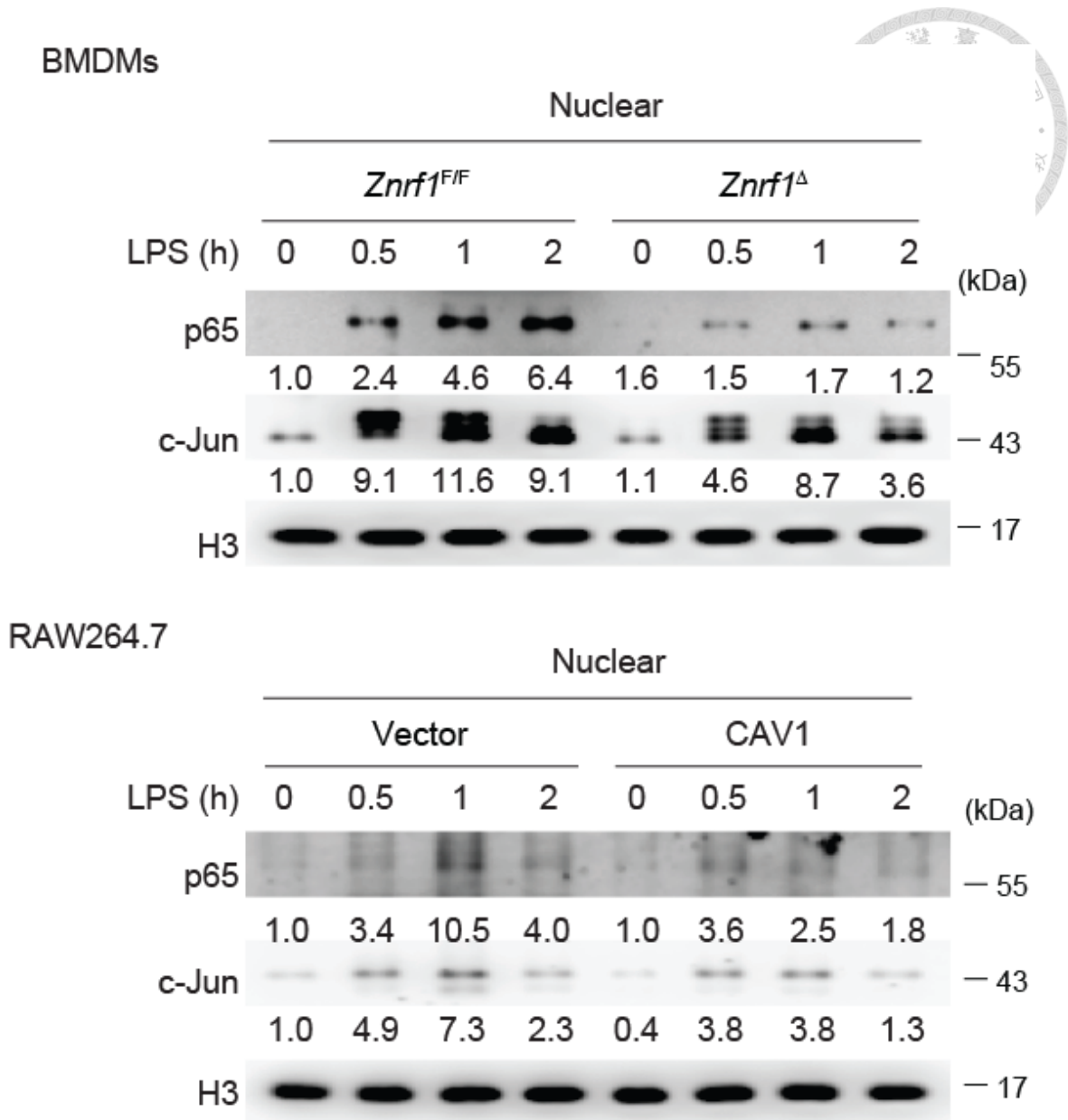
Figure 18. LPS-induced NF-κB activation is decreased in ZNRF1-deficient and CAV1-expressing macrophages.

Immunoblot analysis of NF-κB p65 and c-Jun in nuclear extracts isolated from BMDMs and RAW264.7 cells as described above. Histone H3 served as a marker for the nuclear fraction. The intensities of the bands are shown as fold increases compared to those of untreated control cells after normalization to their unphosphorylated forms or H3 expression.
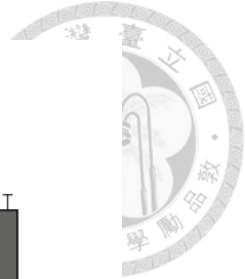
A
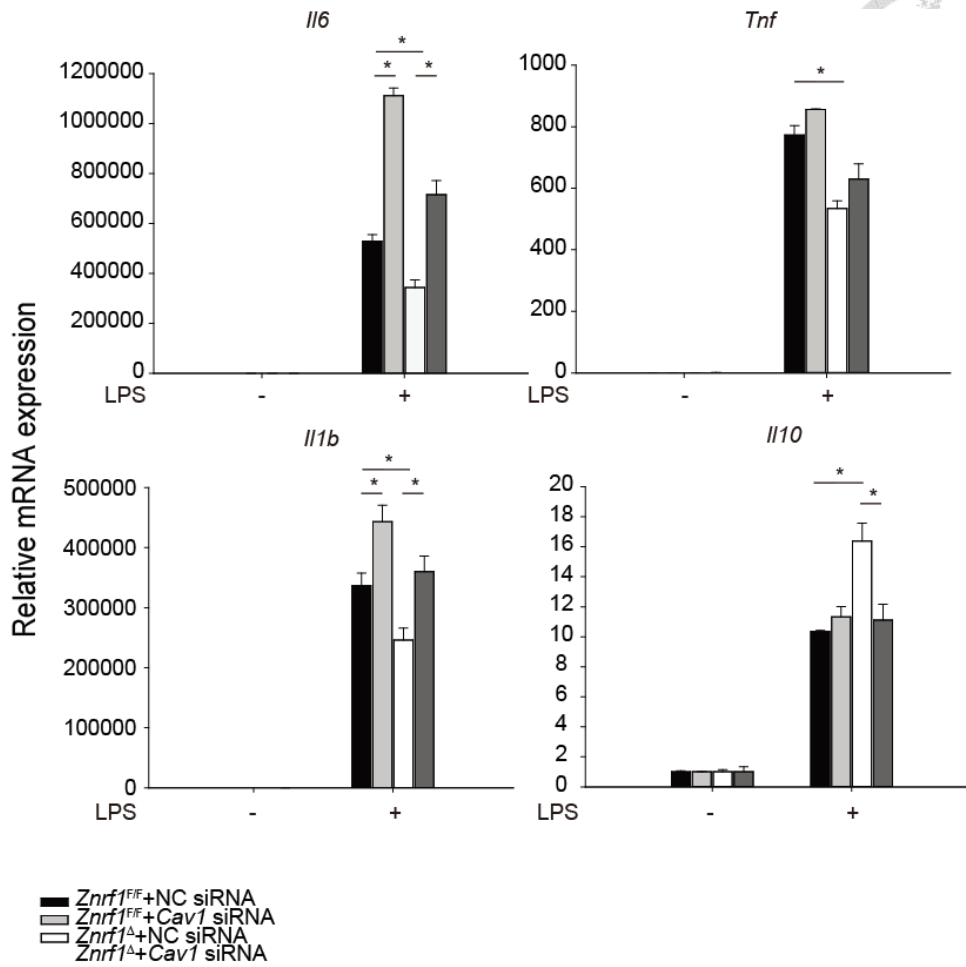
B
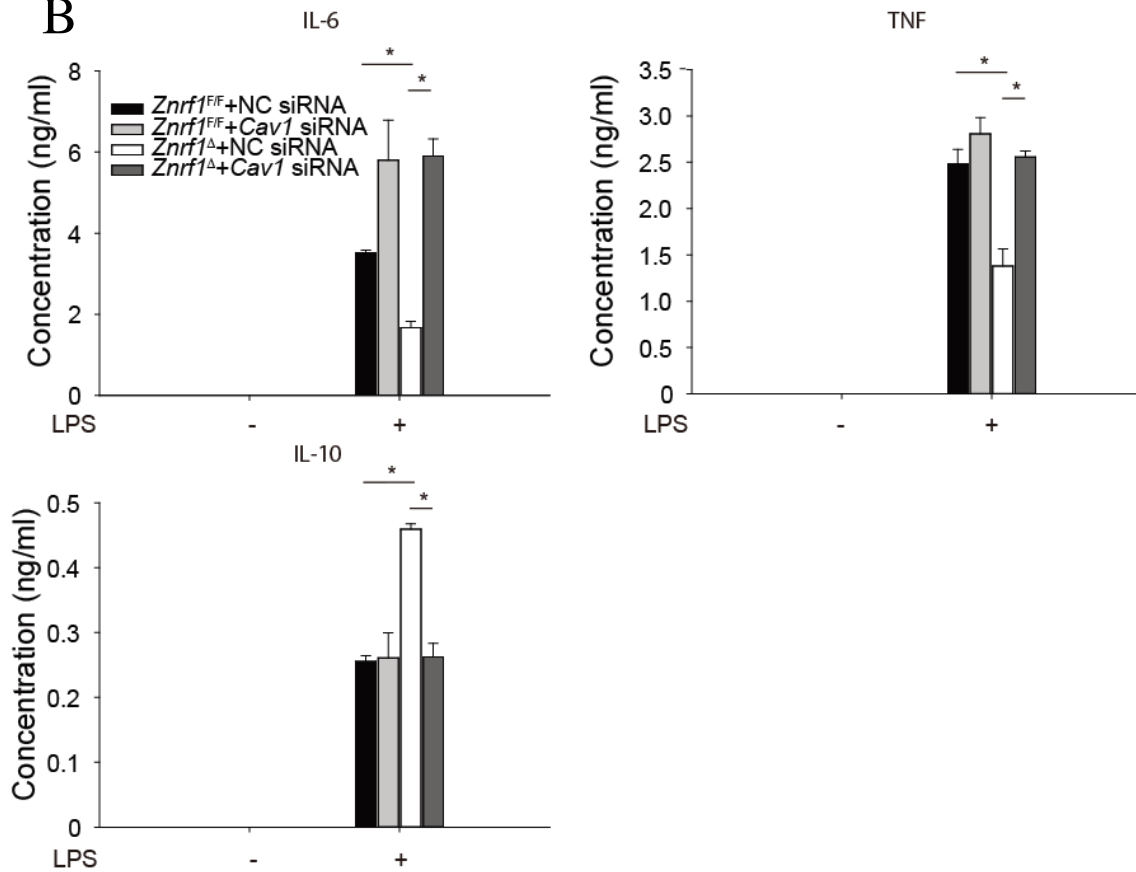
Figure 19. Deletion of CAV1 in ZNRF1-null macrophages restores LPS-induced cytokine expression.

(A-B) *Znrf1*$^{F/F}$ or *Znrf1*$^{\Delta}$ BMDMs electroporated with either control (*NC)* or *Cav1* siRNA were treated with LPS (100 ng/ml). (A) The expression of the indicated mRNAs in BMDMs after stimulation with LPS for 4 hours was analyzed by RT-qPCR. (B) The production of cytokines in culture supernatants of BMDMs 8 hours after treatment with LPS was determined by ELISA. *P<0.05 (Student's *t*-test).

A

	Znrf1^{F/F}+siNC			Znrf1^{F/F}+siCav1			Znrf1^{Δ}+siNC			Znrf1^{Δ}+siCav1		
LPS(min)	0	10	30	0	10	30	0	10	30	0	10	30

pAkt Ser473 — 55 (kDa)
1.0 2.9 3.7 1.2 2.0 1.9 1.0 2.6 6.8 1.1 2.3 3.6

Akt — 55

pGSK3β Ser9 — 43
1.0 3.5 3.5 0.9 1.2 1.7 3.1 6.1 4.3 1.2 4.1 2.1

GSK3β — 43

pCREB Ser129 — 43
1.0 0.8 0.5 0.3 0.6 1.5 0.3 0.4 0.3 0.3 1.5 4.1

CREB — 43

CAV1 — 26

ZNRF1 — 26

GAPDH — 34

B

	Znrf1^{F/F}+siNC			Znrf1^{Δ}+siNC			Znrf1^{F/F}+siCav1					Znrf1^{Δ}+siCav1				
	#1	#2	#3	#1	#2	#3	#1	#2	#3	#4	#5	#1	#2	#3	#4	#5	(kDa)

CAV1 — 23

GAPDH — 34

C

IL-6

Concentration (ng/ml)

● Znrf1^{F/F}+NC siRNA
○ Znrf1^{Δ}+NC siRNA
▼ Znrf1^{F/F}+CAV1 siRNA
△ Znrf1^{Δ}+CAV1 siRNA

CLP   -   +

TNF

Concentration (pg/ml)

CLP   -   +

IL-10

Concentration (pg/ml)

CLP   -   +

89

Figure 20. ZNRF1-mediated TLR4- and CLP-triggered inflammatory responses depend on CAV1.

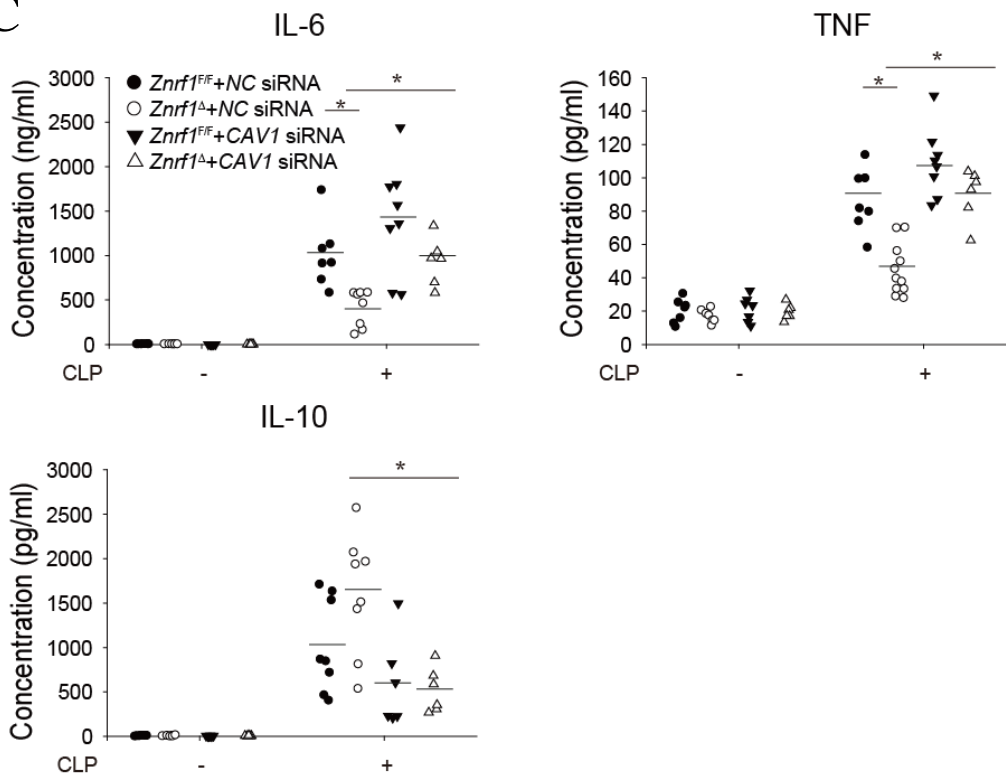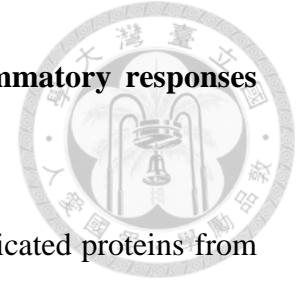(A) Phosphorylation of Akt, GSK3β, and CREB as well as the indicated proteins from BMDM lysates were analyzed by immunoblotting with the indicated antibodies. The data are representative of three independent experiments performed in triplicate (error bars, SD.). (B) $Znrf1^{F/F}$ or $Znrf1^{\Delta}$ mice were injected intravenously with either control (*NC)* or *Cav1* siRNA. After 36 hours, mice were subjected to CLP and white blood cells were collected for immunoblot with indicated antibodies. (C) $Znrf1^{F/F}$ or $Znrf1^{\Delta}$ mice were injected intravenously with either control (*NC*) or *Cav1* siRNA followed by the CLP operation, and blood was collected 8 hours post-CLP. The indicated cytokines in sera were determined by ELISA (bottom), and CAV1 protein levels in peripheral blood leukocytes were analyzed by immunoblotting (top). *P<0.05 (Student's *t*-test).

90
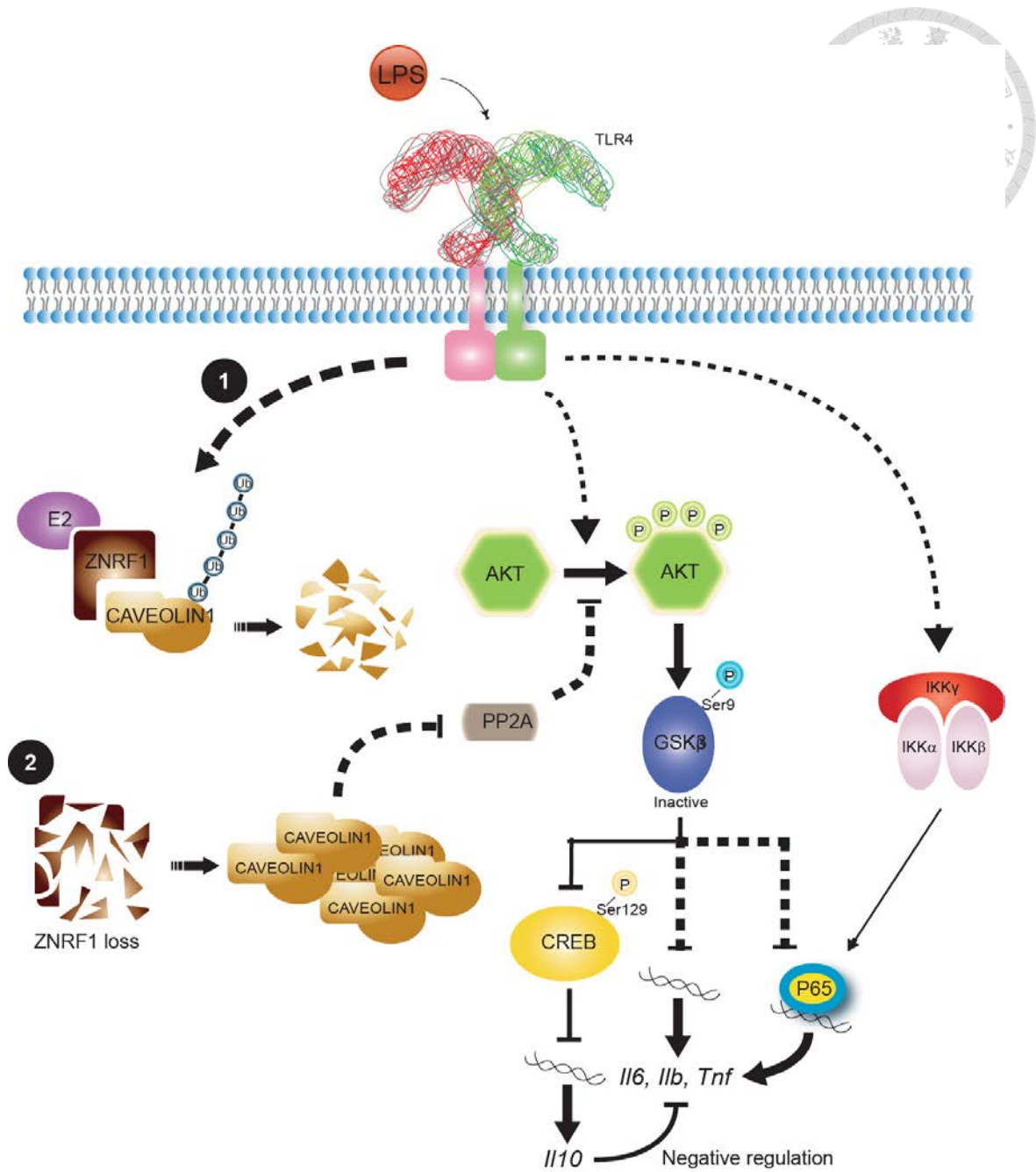
Figure 21. A proposed model summarizing the control of CAV1 protein level and TLR-triggered immune responses by ZNRF1.

TLR4 activation induces an interaction between ZNRF1 and CAV1, which promotes CAV1 ubiquitination and degradation through the proteasome pathway, thereby shifting the balance of the immune response toward increased pro-inflammatory cytokine production. When ZNRF1 is depleted, the elevated expression of CAV1 increases Akt

phosphorylation and activation, resulting in the inactivation of GSK3β by phosphorylation at serine 9. This leads to reduced phosphorylation of CREB serine 129, which results in a substantial increase in IL-10 expression and blocks the production of pro-inflammatory cytokines by suppressing the nuclear translocation of transcription factor NF-κB subunit p65.
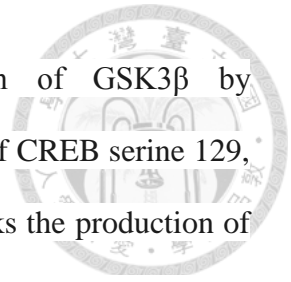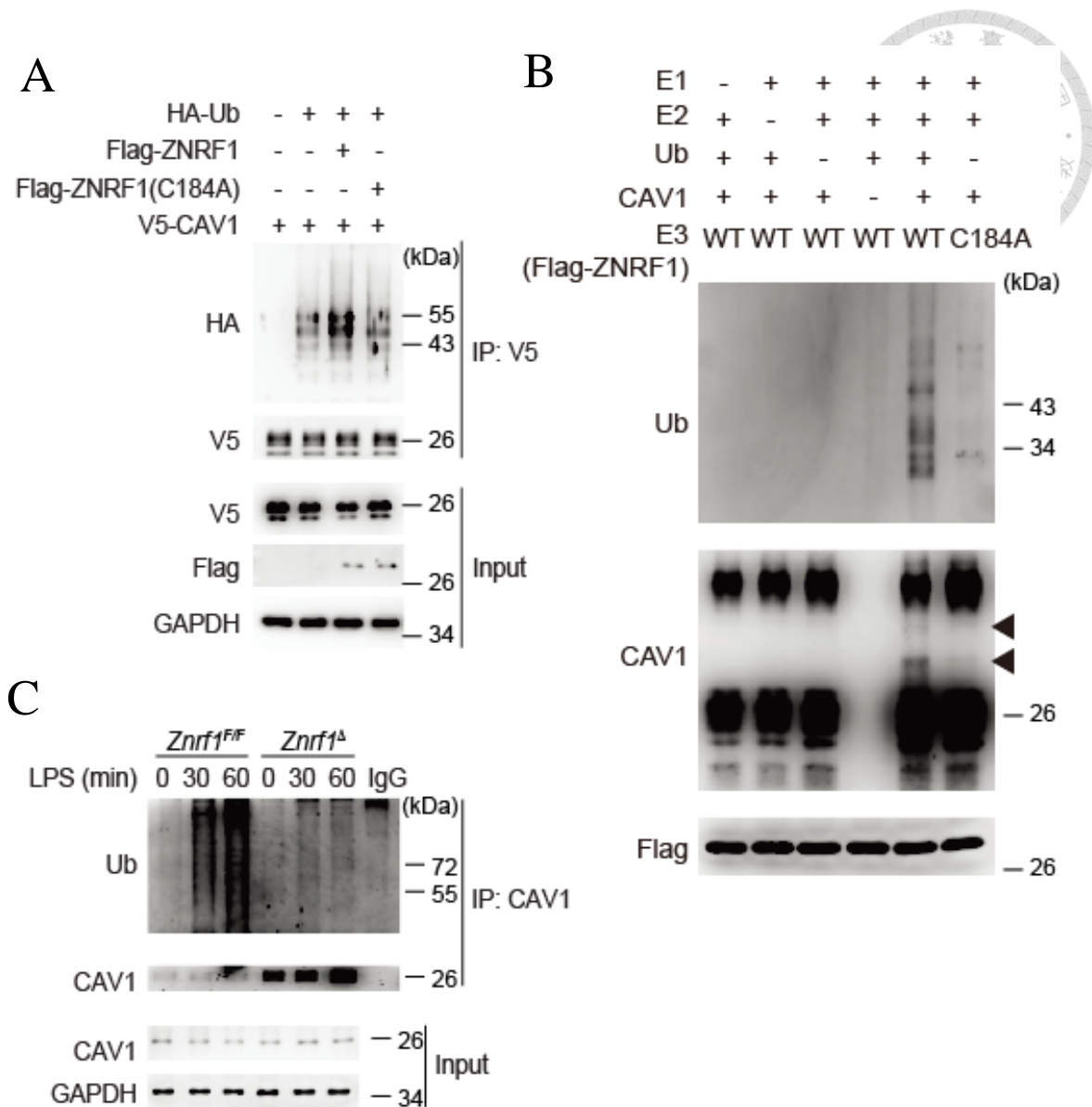
Supplementary Figure 1. The E3 ligase activity of ZNRF1 promotes ubiquitination of CAV1.

(A) HEK293T cells were co-transfected with Flag-tagged ZNRF1 or ZNRF1(C184A) mutant and V5-tagged CAV1 and HA-tagged ubiquitin. CAV1 ubiquitination was determined by immunoprecipitating V5-tagged CAV1 and subsequent immunoblotting with anti-HA. (B) *In vitro* ubiquitination assays were carried out with bacterially expressed His-CAV1, ZNRF1 or ZNRF1(C184A), and purified ubiquitin catalytic components as indicated. The mixtures were then subjected to immunoblotting with the indicated antibodies. Arrows indicate Ubiquitin-conjugated CAV1. (C) BMDMs from

93

Znrf1^F/F and *Znrf1*^Δ mice were treated with LPS (100 ng/ml) for the indicated times after MG132 pre-treatment. CAV1 ubiquitination was determined by immunoprecipitating CAV1 and subsequent immunoblotting with anti-ubiquitin antibody. These data are representative of three independent experiments performed in triplicate.

A
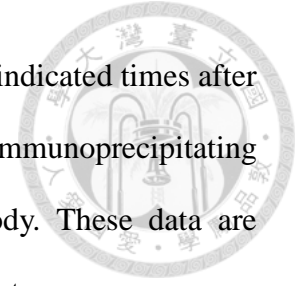
```
              5                     26   30              39           47           57
1  MSGG**K**YVDSEGHLYTVPIREQGNIY**K**PNN**K**AMADEVTE**K**QVYDAHT**K**EIDLVNRDP**K**HLNDDVV
        R                       R     R              R           R           R
      65                            86           96
65 **K**IDFEDVIAEPEGTHSFDGIW**K**ASFTTFTVT**K**YWFYRLLSTIFGIPMALIWGIYFAILSFLHIWAVVP
     R                       R           R
         135                          165          176
133 CI**K**SFLIEIQCISRVYSIYVHTFCDPLFEAIG**K**IFSNIRISTQ**K**EI
       R                              R            R
```

B
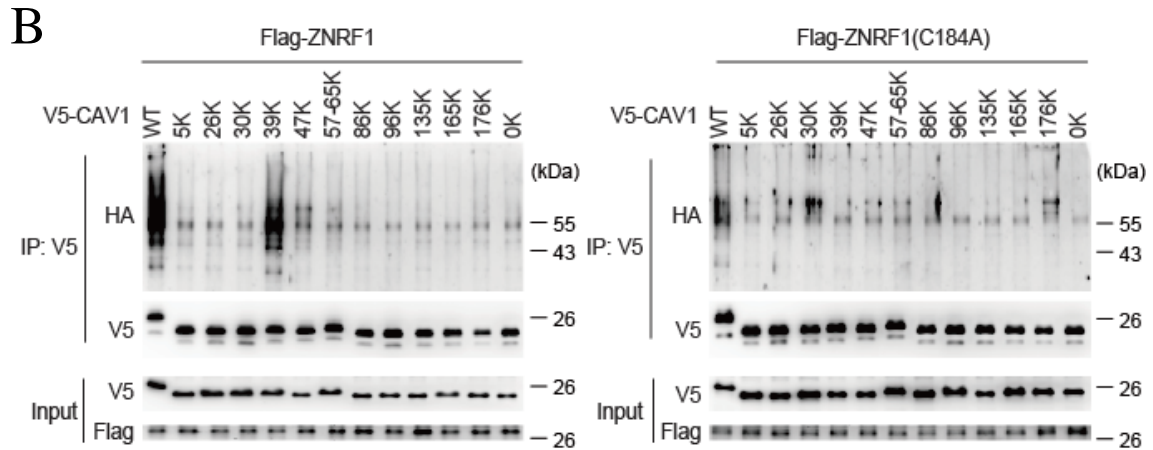
Supplementary Figure 2. ZNRF1 mediates CAV1 polyubiquitination at lysine 39.

(A) Schematic diagram of the mouse CAV1 sequence and its 12 lysine residues, which were mutated to arginines. (B) HEK293T cells were co-transfected with V5-tagged single-lysine CAV1 mutants and either Flag-ZNRF1 or ZNRF1(C184A) as indicated. CAV1 ubiquitination was determined by immunoprecipitating V5-CAV1 and immunoblotting with anti-HA. These data are representative of three independent experiments performed in triplicate.

Reference:

1. Elshabrawy HA, Essani AE, Szekanecz Z, et al. TLRs, future potential
    therapeutic targets for RA. Autoimmun Rev 2016; 9972(16):30267-1.

2. Fatkhullina AR, Peshkova IO, Koltsova EK. The Role of Cytokines in the
    Development of Atherosclerosis. Biochemistry (Mosc) 2016; 81(11):1358-1370.

3. Lin WW, Karin M. A cytokine-mediated link between innate immunity,
    inflammation, and cancer. J Clin Invest 2007; 117(5):1175-83.

4. Liu J, Cao X. Cellular and molecular regulation of innate inflammatory
    responses. Cell Mol Immunol 2016; 13(6):711-721.

5. Hu H, Sun SC. Ubiquitin signaling in immune responses. Cell Res 2016;
    26(4):457-83.

6. Sujashvili R. Advantages of Extracellular Ubiquitin in Modulation of Immune
    Responses. Mediators Inflamm 2016; 2016(4190390):4190390.

7. Liu S, Chen ZJ. Expanding role of ubiquitination in NF-kappaB signaling. Cell
    Res 2011; 21(1):6-21.

8. Cao X. Self-regulation and cross-regulation of pattern-recognition receptor
    signalling in health and disease. Nat Rev Immunol 2016; 16(1):35-50.

9. Kawai T, Akira S. Toll-like receptors and their crosstalk with other innate
    receptors in infection and immunity. Immunity 2011; 34(5):637-50.

10. Kagan JC, Medzhitov R. Phosphoinositide-mediated adaptor recruitment controls Toll-like receptor signaling. Cell 2006; 125(5):943-55.

11. Kawasaki T, Kawai T. Toll-like receptor signaling pathways. Front Immunol 2014; 5(461):461.

12. Watanabe S, Kumazawa Y, Inoue J. Liposomal lipopolysaccharide initiates TRIF-dependent signaling pathway independent of CD14. PLoS One 2013; 8(4):e60078.

13. Pascual-Lucas M, Fernandez-Lizarbe S, Montesinos J, Guerri C. LPS or ethanol triggers clathrin- and rafts/caveolae-dependent endocytosis of TLR4 in cortical astrocytes. J Neurochem 2014; 129(3):448-62.

14. Goldstein G, Scheid M, Hammerling U, et al. Isolation of a polypeptide that has lymphocyte-differentiating properties and is probably represented universally in living cells. Proc Natl Acad Sci U S A 1975; 72(1):11-5.

15. Liu J, Qian C, Cao X. Post-Translational Modification Control of Innate Immunity. Immunity 2016; 45(1):15-30.

16. Li W, Bengtson MH, Ulbrich A, et al. Genome-wide and functional annotation of human E3 ubiquitin ligases identifies MULAN, a mitochondrial E3 that regulates the organelle's dynamics and signaling. PLoS One 2008; 3(1):e1487.

17. Berndsen CE, Wolberger C. New insights into ubiquitin E3 ligase mechanism.

97

Nat Struct Mol Biol 2014; 21(4):301-7.

18. Deshaies RJ, Joazeiro CA. RING domain E3 ubiquitin ligases. Annu Rev Biochem 2009; 78:399-434.

19. Kim HC, Huibregtse JM. Polyubiquitination by HECT E3s and the determinants of chain type specificity. Mol Cell Biol 2009; 29(12):3307-18.

20. Huibregtse JM, Scheffner M, Beaudenon S, Howley PM. A family of proteins structurally and functionally related to the E6-AP ubiquitin-protein ligase. Proc Natl Acad Sci U S A 1995; 92(11):5249.

21. Wenzel DM, Klevit RE. Following Ariadne's thread: a new perspective on RBR ubiquitin ligases. BMC Biol 2012; 10(24):24.

22. Pickart CM. Mechanisms underlying ubiquitination. Annu Rev Biochem 2001; 70:503-33.

23. Koegl M, Hoppe T, Schlenker S, et al. A novel ubiquitination factor, E4, is involved in multiubiquitin chain assembly. Cell 1999; 96(5):635-44.

24. Aravind L, Koonin EV. The U box is a modified RING finger - a common domain in ubiquitination. Curr Biol 2000; 10(4):R132-4.

25. Joazeiro CA, Wing SS, Huang H, et al. The tyrosine kinase negative regulator c-Cbl as a RING-type, E2-dependent ubiquitin-protein ligase. Science 1999; 286(5438):309-12.

26. van der Reijden BA, Erpelinck-Verschueren CA, Lowenberg B, Jansen JH. TRIADs: a new class of proteins with a novel cysteine-rich signature. Protein Sci 1999; 8(7):1557-61.

27. Eisenhaber B, Chumak N, Eisenhaber F, Hauser MT. The ring between ring fingers (RBR) protein family. Genome Biol 2007; 8(3):209.

28. Groettrup M, Pelzer C, Schmidtke G, Hofmann K. Activating the ubiquitin family: UBA6 challenges the field. Trends Biochem Sci 2008; 33(5):230-7.

29. Shin JS, Ebersold M, Pypaert M, et al. Surface expression of MHC class II in dendritic cells is controlled by regulated ubiquitination. Nature 2006; 444(7115):115-8.

30. Baravalle G, Park H, McSweeney M, et al. Ubiquitination of CD86 is a key mechanism in regulating antigen presentation by dendritic cells. J Immunol 2011; 187(6):2966-73.

31. van Niel G, Wubbolts R, Ten Broeke T, et al. Dendritic cells regulate exposure of MHC class II at their plasma membrane by oligoubiquitination. Immunity 2006; 25(6):885-94.

32. Kawai T, Akira S. The role of pattern-recognition receptors in innate immunity: update on Toll-like receptors. Nat Immunol 2010; 11(5):373-84.

33. McWhirter SM, Fitzgerald KA, Rosains J, et al. IFN-regulatory factor
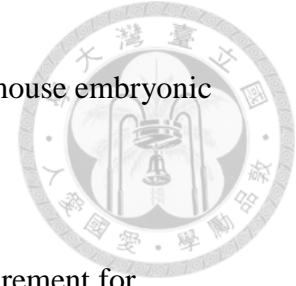
3-dependent gene expression is defective in Tbk1-deficient mouse embryonic

fibroblasts. Proc Natl Acad Sci U S A 2004; 101(1):233-8.

34.   Perry AK, Chow EK, Goodnough JB, et al. Differential requirement for

TANK-binding kinase-1 in type I interferon responses to toll-like receptor

activation and viral infection. J Exp Med 2004; 199(12):1651-8.

35.   Araki T, Nagarajan R, Milbrandt J. Identification of genes induced in peripheral

nerve after injury. Expression profiling and novel gene discovery. J Biol Chem

2001; 276(36):34131-41.

36.   Borden KL. RING fingers and B-boxes: zinc-binding protein-protein interaction

domains. Biochem Cell Biol 1998; 76(2-3):351-8.

37.   Araki T, Milbrandt J. ZNRF proteins constitute a family of presynaptic E3

ubiquitin ligases. J Neurosci 2003; 23(28):9385-94.

38.   Wakatsuki S, Furuno A, Ohshima M, Araki T. Oxidative stress-dependent

phosphorylation activates ZNRF1 to induce neuronal/axonal degeneration. J Cell

Biol 2015; 211(4):881-96.

39.   Wakatsuki S, Araki T. NADPH oxidases promote apoptosis by activating

ZNRF1 ubiquitin ligase in neurons treated with an exogenously applied oxidant.

Commun Integr Biol 2016; 9(2):e1143575.

40.   Hoxhaj G, Najafov A, Toth R, et al. ZNRF2 is released from membranes by
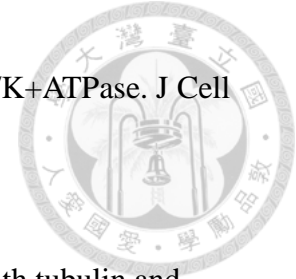
growth factors and, together with ZNRF1, regulates the Na+/K+ATPase. J Cell

Sci 2012; 125(Pt 19):4662-75.

41. Yoshida K, Watanabe M, Hatakeyama S. ZNRF1 interacts with tubulin and

regulates cell morphogenesis. Biochem Biophys Res Commun 2009;

389(3):506-11.

42. Shvets E, Ludwig A, Nichols BJ. News from the caves: update on the structure

and function of caveolae. Curr Opin Cell Biol 2014; 29:99-106.

43. Parton RG, del Pozo MA. Caveolae as plasma membrane sensors, protectors and

organizers. Nat Rev Mol Cell Biol 2013; 14(2):98-112.

44. Feng H, Guo W, Han J, Li XA. Role of caveolin-1 and caveolae signaling in

endotoxemia and sepsis. Life Sci 2013; 93(1):1-6.

45. Vallejo J, Hardin CD. Expression of caveolin-1 in lymphocytes induces caveolae

formation and recruitment of phosphofructokinase to the plasma membrane.

FASEB J 2005; 19(6):586-7.

46. Harris J, Werling D, Hope JC, et al. Caveolae and caveolin in immune cells:

distribution and functions. Trends Immunol 2002; 23(3):158-64.

47. Manes S, del Real G, Martinez AC. Pathogens: raft hijackers. Nat Rev Immunol

2003; 3(7):557-68.

48. Koseki M, Hirano K, Masuda D, et al. Increased lipid rafts and accelerated

lipopolysaccharide-induced tumor necrosis factor-alpha secretion in

Abca1-deficient macrophages. J Lipid Res 2007; 48(2):299-306.

49.   Wang XM, Kim HP, Song R, Choi AM. Caveolin-1 confers antiinflammatory

effects in murine macrophages via the MKK3/p38 MAPK pathway. Am J Respir

Cell Mol Biol 2006; 34(4):434-42.

50.   Lei MG, Morrison DC. Differential expression of caveolin-1 in

lipopolysaccharide-activated murine macrophages. Infect Immun 2000;

68(9):5084-9.

51.   Kuhn R, Schwenk F, Aguet M, Rajewsky K. Inducible gene targeting in mice.

Science 1995; 269(5229):1427-9.

52.   Rittirsch D, Huber-Lang MS, Flierl MA, Ward PA. Immunodesign of

experimental sepsis by cecal ligation and puncture. Nat Protoc 2009; 4(1):31-6.

53.   Hsu LC, Enzler T, Seita J, et al. IL-1beta-driven neutrophilia preserves

antibacterial defense in the absence of the kinase IKKbeta. Nat Immunol 2011;

12(2):144-50.

54.   Ayala A, Perrin MM, Kisala JM, et al. Polymicrobial sepsis selectively activates

peritoneal but not alveolar macrophages to release inflammatory mediators

(interleukins-1 and -6 and tumor necrosis factor). Circ Shock 1992; 36(3):191-9.

55.   Shin JS, Gao Z, Abraham SN. Involvement of cellular caveolae in bacterial entry

into mast cells. Science 2000; 289(5480):785-8.

56.　Akira S. Toll-like receptor signaling. J Biol Chem 2003; 278(40):38105-8.

57.　Wakatsuki S, Saitoh F, Araki T. ZNRF1 promotes Wallerian degeneration by

degrading AKT to induce GSK3B-dependent CRMP2 phosphorylation. Nat Cell

Biol 2011; 13(12):1415-23.

58.　Kirchner P, Bug M, Meyer H. Ubiquitination of the N-terminal region of

caveolin-1 regulates endosomal sorting by the VCP/p97 AAA-ATPase. J Biol

Chem 2013; 288(10):7363-72.

59.　Hayer A, Stoeber M, Ritz D, et al. Caveolin-1 is ubiquitinated and targeted to

intralumenal vesicles in endolysosomes for degradation. J Cell Biol 2010;

191(3):615-29.

60.　Li L, Ren CH, Tahir SA, et al. Caveolin-1 Maintains Activated Akt in Prostate

Cancer Cells through Scaffolding Domain Binding Site Interactions with and

Inhibition of Serine/Threonine Protein Phosphatases PP1 and PP2A. Molecular

and Cellular Biology 2003; 23(24):9389-9404.

61.　Woodgett JR, Ohashi PS. GSK3: an in-Toll-erant protein kinase? Nat Immunol

2005; 6(8):751-2.

62.　Martin M, Rehani K, Jope RS, Michalek SM. Toll-like receptor-mediated

cytokine production is differentially regulated by glycogen synthase kinase 3.

103

Nat Immunol 2005; 6(8):777-84.

63. Platzer C, Fritsch E, Elsner T, et al. Cyclic adenosine monophosphate-responsive

elements are involved in the transcriptional activation of the human IL-10 gene

in monocytic cells. Eur J Immunol 1999; 29(10):3098-104.

64. Takeuchi O, Akira S. Pattern recognition receptors and inflammation. Cell 2010;

140(6):805-20.

65. Mirza MK, Yuan J, Gao XP, et al. Caveolin-1 deficiency dampens Toll-like

receptor 4 signaling through eNOS activation. Am J Pathol 2010;

176(5):2344-51.

66. Jiao H, Zhang Y, Yan Z, et al. Caveolin-1 Tyr14 phosphorylation induces

interaction with TLR4 in endothelial cells and mediates MyD88-dependent

signaling and sepsis-induced lung inflammation. J Immunol 2013;

191(12):6191-9.

67. Iyer SS, Ghaffari AA, Cheng G. Lipopolysaccharide-Mediated IL-10

Transcriptional Regulation Requires Sequential Induction of Type I IFNs and

IL-27 in Macrophages. The Journal of Immunology 2010; 185(11):6599-6607.

68. Saraiva M, O'Garra A. The regulation of IL-10 production by immune cells. Nat

Rev Immunol 2010; 10(3):170-181.

69. Cohen P, Frame S. The renaissance of GSK3. Nat Rev Mol Cell Biol 2001;

2(10):769-776.

70.   Simmons GE, Jr., Taylor HE, Hildreth JE. Caveolin-1 suppresses human

immunodeficiency virus-1 replication by inhibiting acetylation of NF-kappaB.

Virology 2012; 432(1):110-9.

71.   Zuluaga S, lvarez-Barrientos A, Gutiérrez-Uzquiza A, et al. Negative regulation

of Akt activity by p38α MAP kinase in cardiomyocytes involves membrane

localization of PP2A through interaction with caveolin-1. Cell Signal 2007;

19(1):62-74.

72.   Henkhaus RS, Roy UKB, Cavallo-Medved D, et al. Caveolin-1-Mediated

Expression and Secretion of Kallikrein 6 in Colon Cancer Cells. Neoplasia 2008;

10(2):140-148.

73.   Aksoy E, Taboubi S, Torres D, et al. The p110delta isoform of the kinase PI(3)K

controls the subcellular compartmentalization of TLR4 signaling and protects

from endotoxic shock. Nat Immunol 2012; 13(11):1045-54.

74.   Lei MG, Tan X, Qureshi N, Morrison DC. Regulation of cellular caveolin-1

protein expression in murine macrophages by microbial products. Infect Immun

2005; 73(12):8136-43.